

Achieving High Reliability Low Cost Lead-Free SAC Solder Joints Via Mn Or Ce Doping

Dr. Weiping Liu¹, Dr. Ning-Cheng Lee¹, Adriana Porras², Dr. Min Ding², Anthony Gallagher³, Austin Huang⁴, Scott Chen⁴, and Jeffrey ChangBing Lee⁵

1 Indium Corporation

2 Freescale Semiconductor

3 Motorola Inc

4 Advanced Semiconductor Engineering Group

5 IST-Integrated Service Technology Inc

Abstract

In this study, the reliabilities of low Ag SAC alloys doped with Mn or Ce (SACM or SACC) were evaluated under JEDEC drop, dynamic bending, thermal cycling, and cyclic bending test conditions against eutectic SnPb, SAC105, and SAC305 alloys. The Mn or Ce doped low cost SAC105 alloys achieved a higher drop test and dynamic bending test reliability than SAC105 and SAC305, and exceeded SnPb for some test conditions. More significantly, being a slightly doped SAC105, both SACM and SACC matched SAC305 in thermal cycling performance. In other words, the low cost SACM and SACC achieved a better drop test performance than the low Ag SAC alloys plus the desired thermal cycling reliability of high Ag SAC alloys. The mechanism for high drop performance and high thermal cycling reliability can be attributed to a stabilized microstructure, with uniform distribution of fine IMC particles, presumably through the inclusion of Mn or Ce in the IMC. The cyclic bending results showed SAC305 being the best, and all lead-free alloys are equal or superior to SnPb. The reliability test results also showed that NiAu is a preferred surface finish for BGA packages over OSP.

Key Words

Lead-free, solder, SnAgCu, SAC, Mn, Ce, reliability, drop, thermal cycling, bending

Introduction

Lead-free soldering has been widely adopted by the electronics industry, with SnAgCu (SAC) having high Ag content being the initial main stream of choice. This selection was challenged later by the fragility of solder joint toward drop and the high cost of Ag. Low Ag SAC was considered a solution for resolving both issues. However, this approach compromised temperature cycling performance, therefore is not acceptable for high end applications. In this study, low Ag SAC alloys doped with Mn or Ce were evaluated against eutectic SnPb, SAC105, and SAC305 for JEDEC drop, dynamic bending test, -40/125°C temperature cycling, and 1Hz/2mm cyclic bending tests. Prior to the drop and bending tests, a part of the samples were preconditioned with 150°C thermal aging or 250 cycles temperature cycling. The primary test vehicle employed was TFBGA with NiAu finish mounted on PCB with OSP finish.

Experiment

1. Assembly

(1) Solder Alloys:

Five solder sphere alloys were evaluated, including two new alloys, 98.5Sn1Ag0.5Cu0.05Mn (SACM) and 98.5Sn1Ag0.5Cu0.02Ce (SACC), and three controls, 63Sn37Pb (SnPb), 98.5Sn1Ag0.5Cu (SAC105), and 96.5Sn3Ag0.5Cu (SAC305).

For JEDEC drop test, thermal cycling test, and cyclic bending test, two no-clean solder pastes were used, SnPb and SAC305. The former was used for SnPb TFBGA mounting, while the latter was for lead-free TFBGA mounting.

For dynamic bending test, 95.5Sn3.8Ag0.7Cu (SAC387) no-clean solder paste was used.

(2) Device Assembly:

For JEDEC drop test, temperature cycling test, and cyclic bending test, the following parts and reflow profiles were used.

Components: Daisy TFBGA244, 12X12, 0.3 mm ball/0.5 mm pitch, electrolytic NiAu (5 μ Ni and 0.2-0.5 μ Au), and OSP (0.2-0.4 μ). Unless otherwise specified, all work was done on NiAu.

PCB: High Tg FR4/8 layers/Non-Via In Pad (NVID)/Non-Solder Mask-Defined Pad (NSMD), with surface finishes of organic solderability preservative (OSP, 0.2-0.4 μ), electroless nickel immersion gold (ENIG, with 5 μ Ni and 0.1 μ Au), and Immersion silver (ImAg, 0.2 μ). Unless otherwise specified, all work was done on OSP.
 Reflow profile for SnPb assembly: peak temperature 220°C, reflow under air.
 Reflow profile for lead-free assembly: peak temperature 245°C, reflow under air.

For dynamic bending test, the following parts and reflow profile were used.

Components: Live TFBGA244, 12X12, 0.3 mm ball/0.5 mm pitch, electrolytic NiAu (5 μ Ni and 0.2-0.5 μ Au)
 PCB: FR4/8 layer/NVIP/Solder Mask-Defined Pad (SMD), with OSP finish (0.2-0.4 μ).
 Reflow profile: ramp-to-peak, peak temperature 235°C, reflow under air.

2. Tests

Four tests were conducted in the evaluation of the solder materials.

(1) JEDEC Drop Test (JDT)

Fifteen packages were mounted on a 132 x 77 x 1 mm³ standard 8-layer JEDEC drop test board in a layout regulated by JEDEC, in which the mounted packages were individually numbered. The test board and each of the mounted packages were daisy-chain designed so that the overall electrical resistance of daisy-chained solder joints could be individually measured for each mounted package.

On the test PC board side, the solder joint was in a NSMD structural configuration. The diameter of the OSP coated Cu pad was 0.28 mm whereas the solder mask opening was 0.43 mm, following the requirement of JESD22-B111 for the pitch of solder joints at 0.5 mm.

The drop times were recorded for failed unit when resistance exceeding 1000 ohms.

As schematically shown in Fig. 1, the board-level test vehicle was affixed to the drop table at the four corners with the mounted packages facing downward, according to the regulation by JESD22-B111. The drop table was then released and dropped freely at a certain height to impact on the strike surface repetitively, each time creating a half-sine impact acceleration pulse of a peak acceleration of G_0 (1500Gs) and duration of τ (0.5 ms). Before each test the tightness of the test board should be checked to avoid experimental uncertainties as a result of extra vibrations of the board.

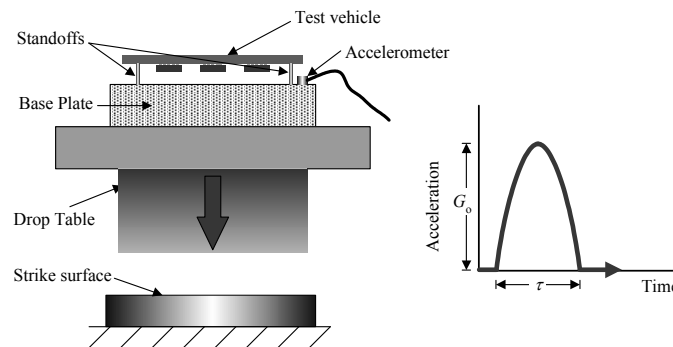


Fig. 1 Schematic for JEDEC board-level drop test.

(2) Thermal Cycling Test (TCT)

The samples were subject to TCT (-40~125°C, 42 min/cycle, ramp up/down: 11 min, dwell time 10 min) with real time resistance monitoring. A failure was defined when a 20% resistance increase was recorded.

(3) Cyclic Bending Test (CBT)

Nine packages were mounted on a 132x77x1 mm³ standard 8-layer PC board with layout regulated by JESD22B113, as shown in the figure where the mounted package were numbered individually. The test board and mounted package was daisy-chain designed so that the overall electrical resistance of daisy-chain solders joints can be individually measured in each mounted package. Each cell was subject to cyclic bend test at 1 Hz/2mm testing condition until all components failure and the cycles number were recorded for failed unit when resistance exceeding 1000 ohms.

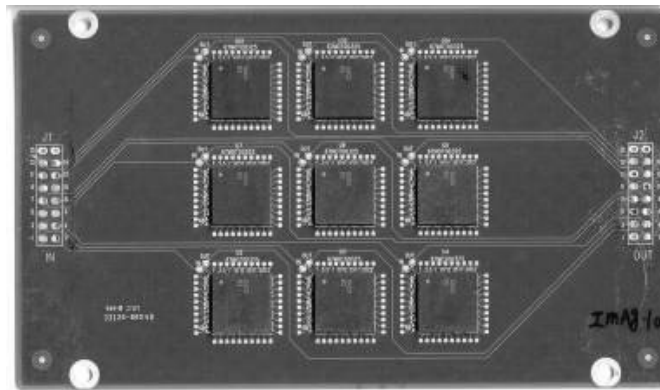


Fig. 2 Board level cyclic bend test vehicle

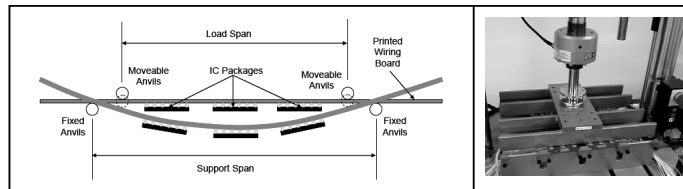


Fig.3 Schematic showing 4-Point bending set-up & machine

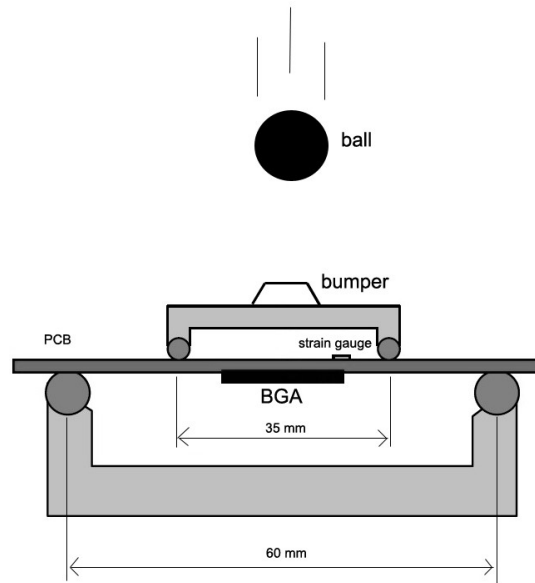


Fig. 4 High strain rate 4 point dynamic bending setup

(4) Dynamic Bending Test (DBT)

A high strain rate drop test reported by Motorola [1-3] was adopted in this work to measure failure behavior of the second-level package reliability for mobile applications. This test was found to regenerate the failure mode of solder joints in surface mount devices found in the phone drop [4].

The test apparatus was composed of the 4-point bending setup. During testing the bending direction by connecting two opposite corner balls of the device was aligned along the longitudinal direction of the PCB. The rollers of the bottom span of the 4-point bending fixture were positioned 60 mm apart while the top span distance was 35 mm. A steel ball was dropped from various heights onto the top span fixture to induce various levels of strains in order to control stress levels at solder joints. The strain gauge was mounted on the back of the PCB, as shown in Fig. 4.

The board strain was increased incrementally, and each unit was impacted only once. After the dynamic bending test, joint failure was identified by dye and pry process. The number of joint failures for each unit was collected for the given board strains, and the data set was fit to a Weibull curve to obtain the board strain level required to generate one solder joint failure.

Prior to the above tests, the devices were preconditioned with thermal aging at 150°C. Further more, drop test or cyclic bending test after TCT pretreatment was conducted. The DOEs for primary work are shown in Table 1 and Table 2.

Results

1. JEDEC Drop Test (JDT)

For devices with TFBGA (NiAu) assembled on PCB (OSP) pretreated with 250 cycles of TCT, the JDT performance of various sphere alloys is represented in Weibull plot shown in Fig. 5. The reliability can be ranked in the following order:

SACM ≥ SnPb ≥ SACC > SAC105 > SAC305

Fig. 6 and Fig. 7 show the characteristic life (C-Life) and first failure of JDT for TFBGA (NiAu) on PCB (OSP), respectively. Overall, the C-Life of alloys for as reflowed devices is ranked as:

SACC > SACM > SAC105 > SnPb > SAC305

On the other hand, the ranking of alloys on first failure for as reflowed devices is shown below.

Table 1 DOE for JEDEC tests.

Package	Daisy TFBGA244 12X12					
Ball/pitch (mm)	0.3/0.5	0.3/0.5	0.3/0.5	0.3/0.5	0.3/0.5	0.3/0.5
Solder ball	SnPb	SAC105	SAC305	SACM	SACM	SACC
Surface finish of substrate	NiAu	NiAu	NiAu	NiAu	Cu/OSP	NiAu
Solder paste	SnPb	SAC305	SAC305	SAC305	SAC305	SAC305
Reflow profile	220C	245C	245C	245C	245C	245C
PCB	High Tg FR4/8 layer/NVIP/NSMD/OSP					
Thermal aging 150C/0hr	TCT (-40/125) solder joint reliability					
	Drop solder joint reliability					
	Cyclic Bending (1Hz/2mm) solder joint reliability					
Thermal aging 150C/100hr	TCT (-40/125) solder joint reliability					
	Drop solder joint reliability					
	Cyclic Bending (1Hz/2mm) solder joint reliability					
Thermal aging 150C/250hr	TCT (-40/125) solder joint reliability					
	Drop solder joint reliability					
	Cyclic Bending (1Hz/2mm) solder joint reliability					
TCT (-40/125C) 250 cycle	Drop solder joint reliability					
	Cyclic Bending solder joint reliability					
Thermal aging(0/100/250hrs/1000hrs)	X-section view for interfacial IMC microstructure in package and PCB (OSP) side					

Table 2 DOE for 4 point dynamic bending test.

Package		Live TFBGA			
Ball/pitch (mm)		0.3/0.5	0.3/0.5	0.3/0.5	0.3/0.5
Surface finish (substrate)		NiAu	NiAu	NiAu	NiAu
Solder ball		SAC105	SAC305	SACM	SACC
Solder paste		SAC387			
Reflow profile		Mountain profile (235C peak)			
PCB		FR4/8 layer/NVIP/SMD			
Thermal aging 150C/0hr	Dynamic bending	Dye and pry			
Thermal aging 150C/250hr	Dynamic bending	Dye and pry			

SACC > SACM > SnPb > SAC105 > SAC305

For devices which have been thermally aged or temperature

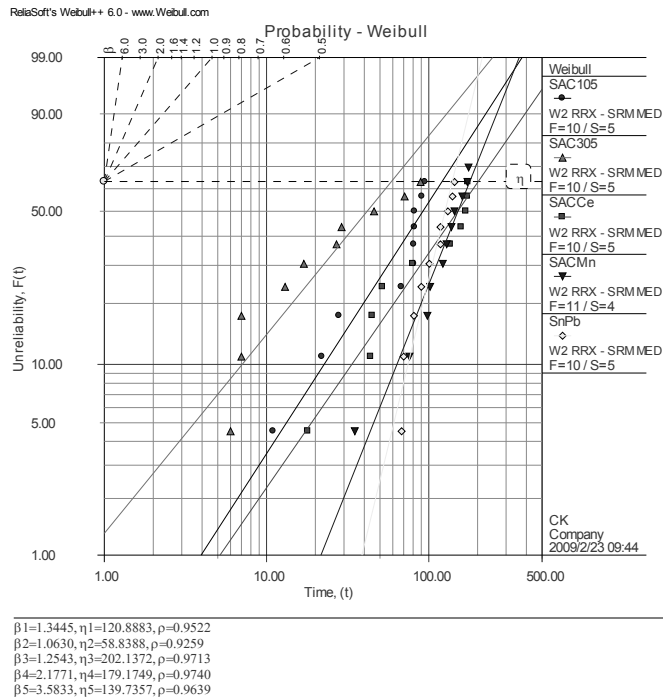


Fig. 5 Weibull plot for JDT performance for TFBGA (NiAu) with various sphere alloys assembled on PCB (OSP). The device was pretreated with 250 cycles of TCT prior to JDT.

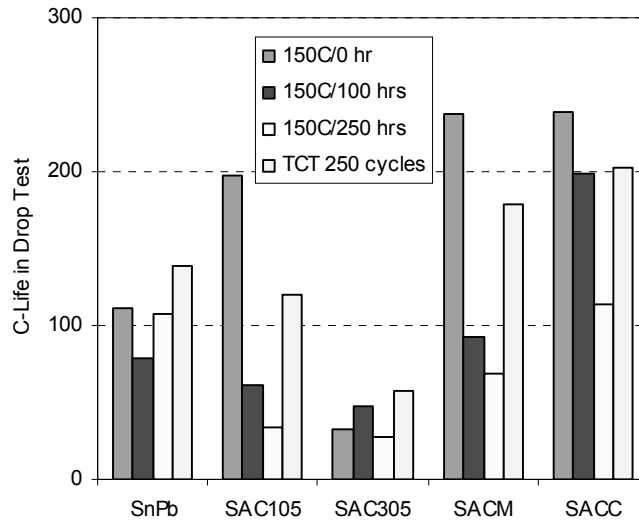


Fig. 6 C-Life in JDT for TFBGA (NiAu) on PCB (OSP) cycled, the ranking of first failure is shown below.

SnPb > SACM > SACC > SAC105 > SAC305

Fig. 8 and Fig. 9 show the effect of package surface finish on the C-Life and first failure of JDT for TFBGA on PCB (OSP), respectively using SACM. Overall, for devices pretreated with

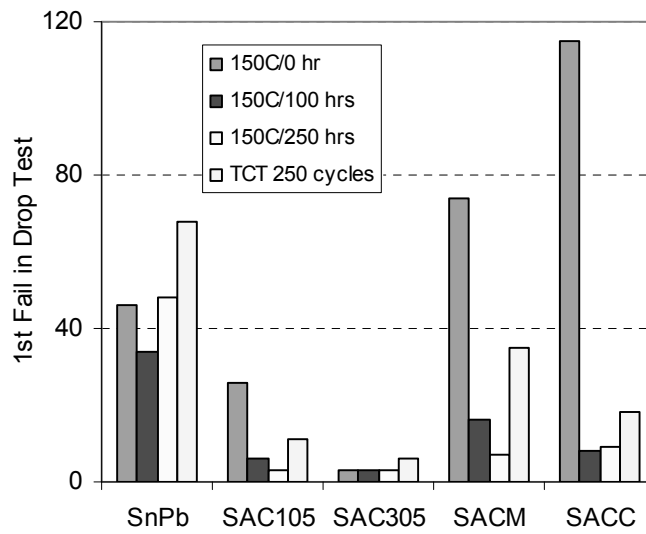


Fig. 7 First Failure in JDT for TFBGA (NiAu) on PCB (OSP)

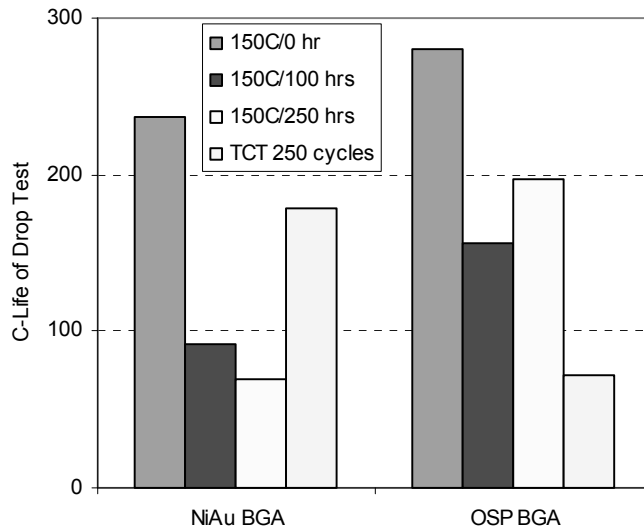


Fig. 8 C-Life in JDT for TFBGA on PCB (OSP) for SACM.

250 TCT, the JDT reliability of NiAu is better than OSP. However, for as reflowed devices or thermally aged devices, the JDT reliability of OSP is better than NiAu.

The effect of PCB surface finishes on JDT was studied for SACM and SACC. Fig. 10 shows the C-Life while Fig. 11 shows the first failure. In most cases, for as reflowed devices, the reliability of JDT shows the following order: ImAg > OSP > ENIG. For thermally aged or thermal cycled devices, the trend slightly changed: OSP > ImAg > ENIG in most instances.

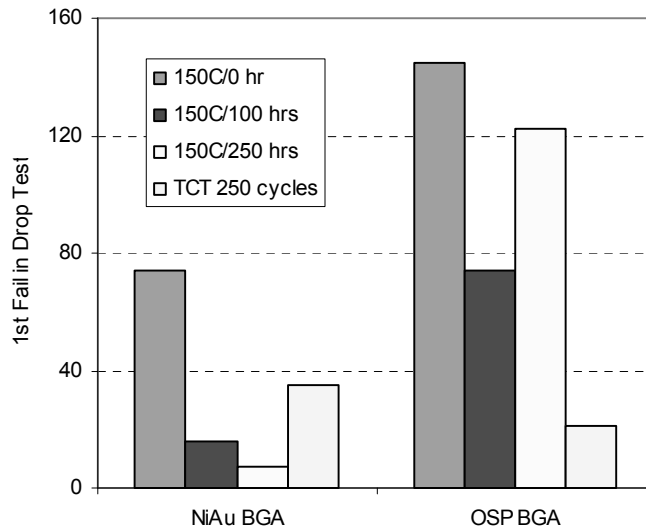


Fig. 9 First failure in JDT for TFBGA on PCB (OSP) for SACM

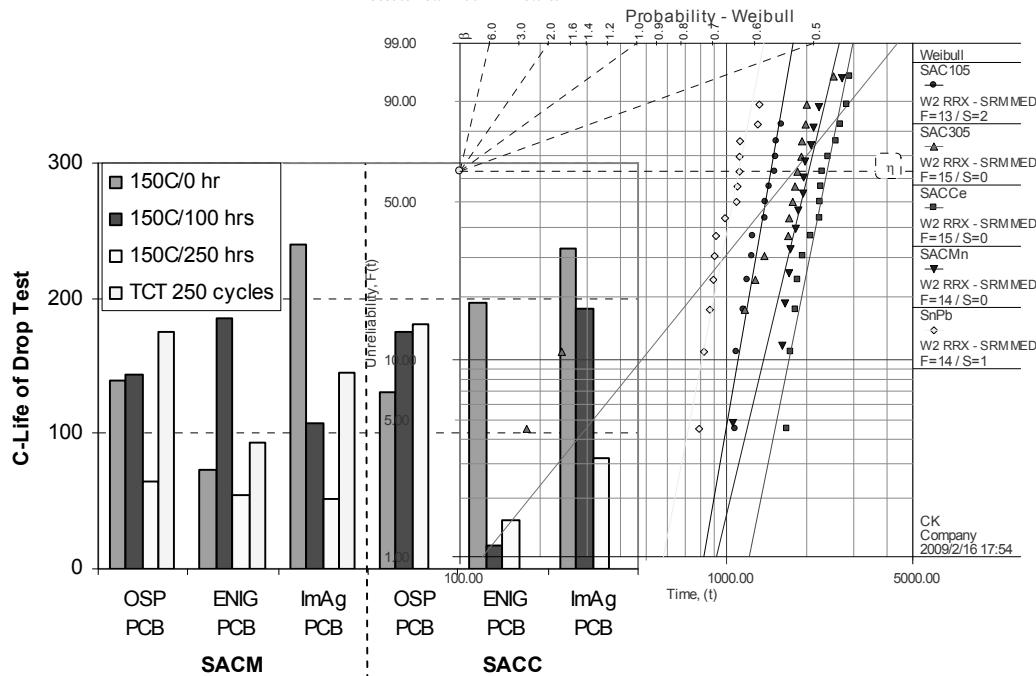


Fig. 10 Effect of PCB surface finish on C-Life of JDT for SACM and SACC for devices assembled with TFBGA (NiAu).

2. Thermal Cycle Test (TCT)

For devices with TFBGA (NiAu) assembled on PCB (OSP) and aged at 150C for 250 hrs, the TCT performance of various sphere alloys is represented in Weibull plot shown in Fig. 12. The reliability can be ranked in the following order: SACC > SACM ≥ SAC305 > SAC105 > SnPb

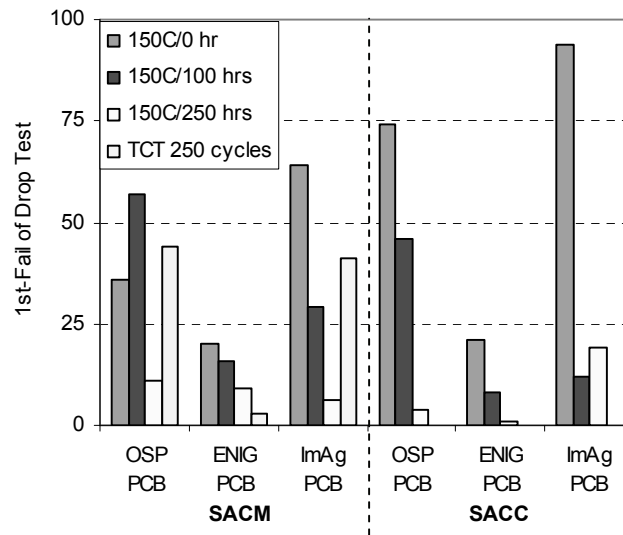


Fig. 11 Effect of PCB surface finish on first failure of JDT for SACM and SACC for devices assembled with TFBGA (NiAu).

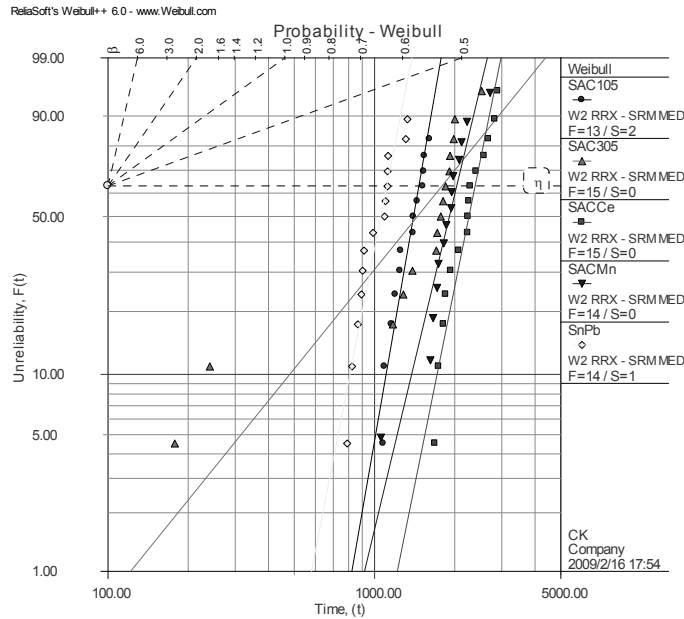


Fig. 12 Weibull plot for TCT performance for TFBGA (NiAu) with various sphere alloys assembled on PCB (OSP). Prior to TCT, the device was aged at 150C for 250 hrs.

Fig. 13 and Fig. 14 show the C-Life and first failure of TCT for TFBGA (NiAu) on PCB (OSP), respectively. Overall, the C-Life of alloys for as reflowed devices can be ranked below.

SAC305 > SACC, SACM > SAC105 > SnPb

However, for devices which have been thermally aged or thermal cycled, the ranking of C-life is shown below.
 SACC ≥ SACM, SAC305 > SAC105 > SnPb

On the other hand, the ranking of alloys on first failure for as reflowed devices is shown below.

SnPb > SACC > SACM > SAC105 > SAC305

For devices which have been thermally aged or thermal cycled, the ranking of first failure is shown below.

SACM > SACC > SAC105 > SnPb > SAC305

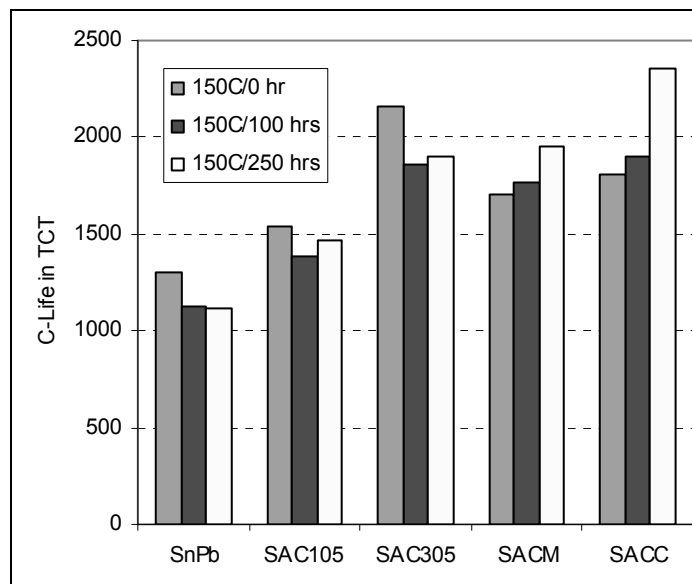


Fig. 13 C-Life of TCT for TFBGA (NiAu) on PCB (OSP).

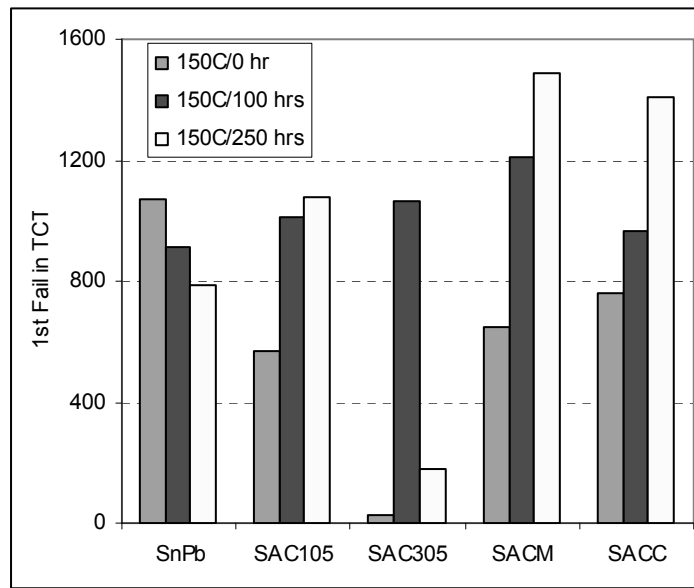


Fig. 14 First failure of TCT for TFBGA (NiAu) on PCB (OSP).

For SACM, the effect of package surface finish type on TCT reliability is shown in Fig. 15 and Fig. 16 for C-Life and first failure, respectively. NiAu is distinctly better than OSP in this case.

The effect of PCB surface finishes on TCT was studied for SACM and SACC. Fig. 17 shows the C-Life while Fig. 18 shows the first failure. ENIG appears to be more noticeably poorer than the other two finishes. Overall, there is a weak trend showing ImAg > OSP > ENIG.

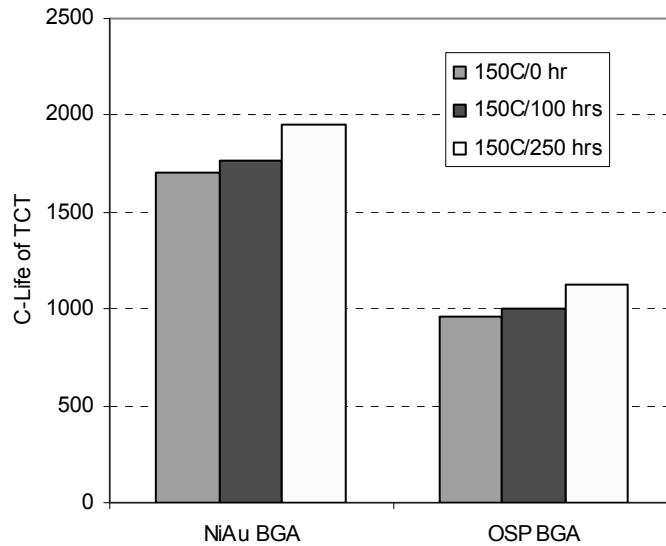


Fig. 15 Effect of TFBGA surface finish on C-Life of TCT for BGA on PCB (OSP) for SACM.

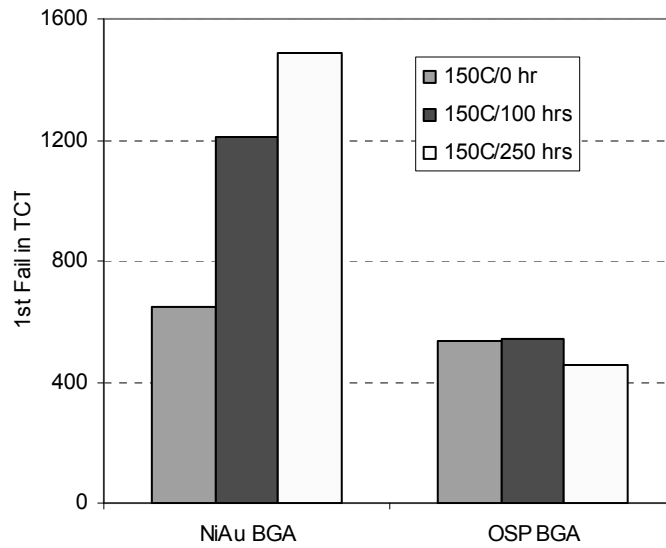


Fig. 16 Effect of TFBGA surface finish on first failure of TCT for BGA on PCB (OSP) for SACM.

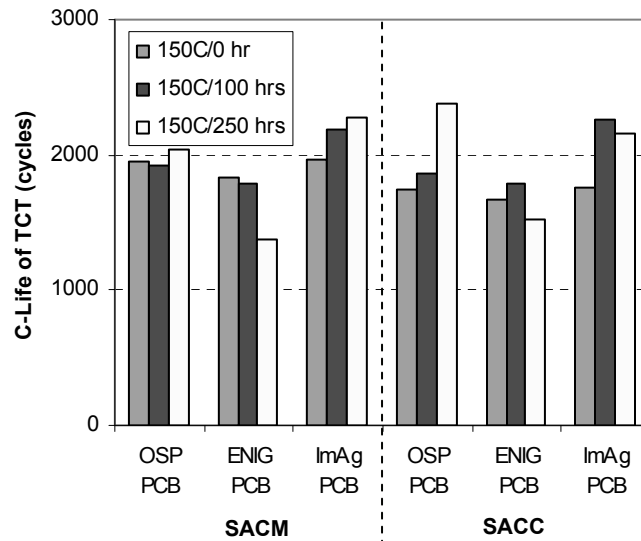


Fig. 17 Effect of PCB surface finish on C-Life of TCT for SACM and SACC for devices assembled with TFBGA (NiAu).

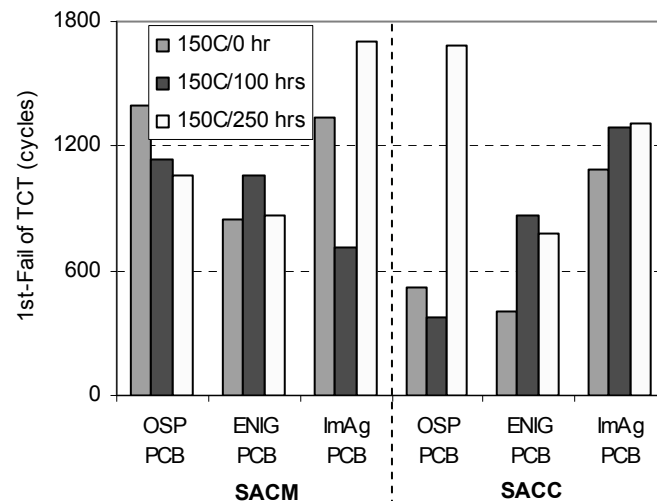


Fig. 18 Effect of PCB surface finish on first failure of TCT for SACM and SACC for devices assembled with TFBGA (NiAu).

3. Cyclic Bending Test (CBT)

For devices with TFBGA (NiAu) assembled on PCB (OSP) and aged at 150°C for 250 hrs, the CBT performance of various sphere alloys is represented in Weibull plot shown in Fig. 19. The reliability can be ranked in the following order:

SAC305 > SACC, SACM, SAC105 > SnPb

Fig. 20 and Fig. 21 show the characteristic life (C-Life) and first failure of CBT for TFBGA (NiAu) on PCB (OSP), respectively. Overall, the C-Life of alloys for as reflowed devices can be ranked below.

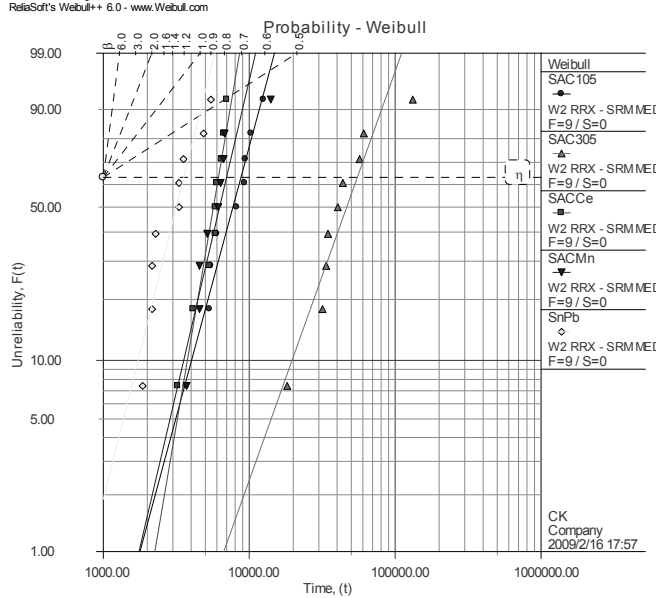


Fig. 19 Weibull plot for CBT performance for as reflowed TFBGA (NiAu) using various sphere alloys assembled on PCB (OSP).

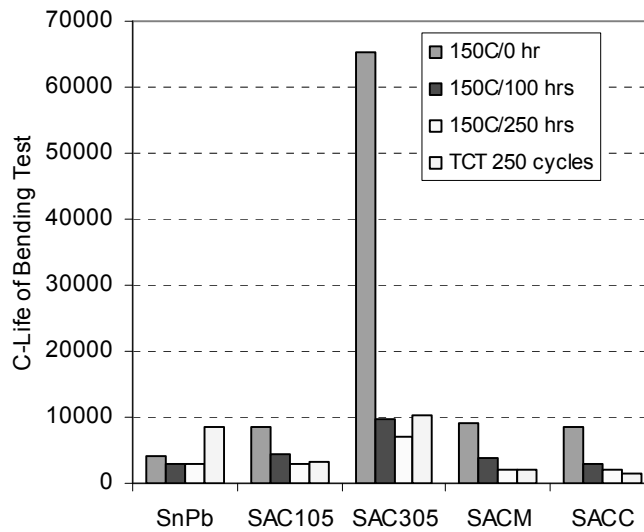


Fig. 20 C-Life of CBT for TFBGA (NiAu) on PCB (OSP)

SAC305 >> SACM ≥ SACC, SAC105 > SnPb

However, for devices which have been thermally aged or temperature cycled, the ranking of C-life is shown below.
SAC305 > SAC105 ≥ SACM, SnPb ≥ SACC

On the other hand, the ranking of alloys on first failure for as reflowed devices is shown below.

SAC305 > SACM > SAC105 ≥ SACC > SnPb

For devices which have been thermally aged or temperature cycled, the ranking of first failure is shown below.

SAC305 > SAC105 > SACM, SnPb > SACC

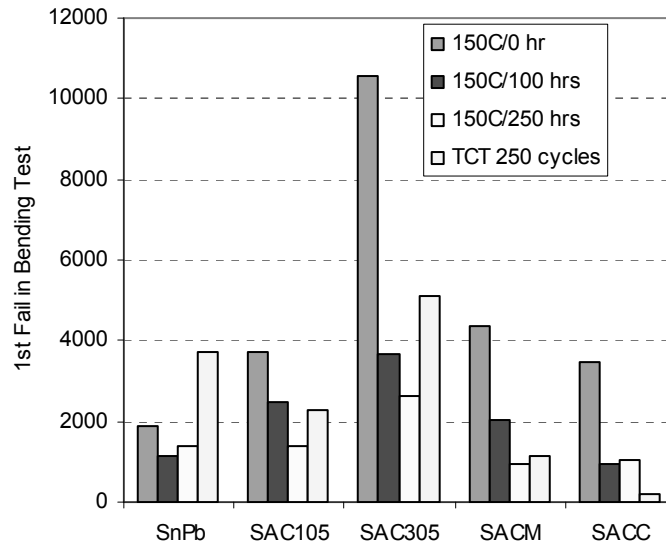


Fig. 21 1st Fail of CBT for TFBGA (NiAu) on PCB (OSP)

For SACM, the effect of package surface finish type on CBT reliability is shown in Fig. 22 and Fig. 23 for C-Life and first failure, respectively. For as reflowed or thermal cycled devices, NiAu is better than OSP. The trend vanishes for thermally aged devices.

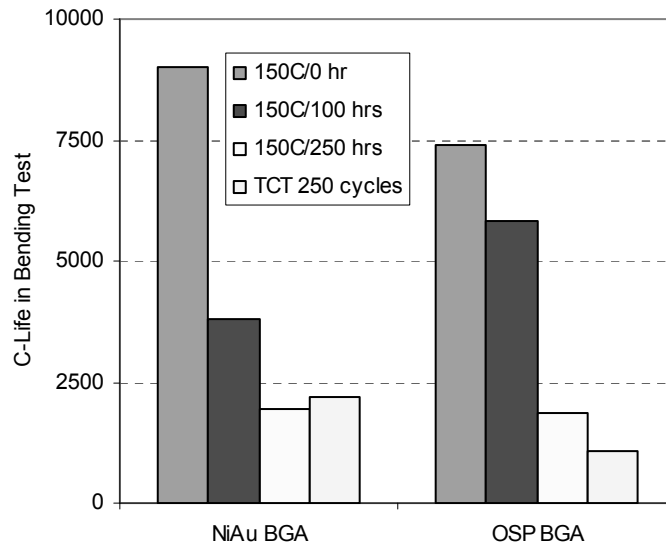


Fig. 22 Effect of TFBGA surface finish on C-Life of CBT for BGA on PCB (OSP) for SACM.

The effect of PCB surface finishes on CBT was studied for SACM and SACC. Fig. 24 shows the C-Life while Fig. 25 shows the first failure.

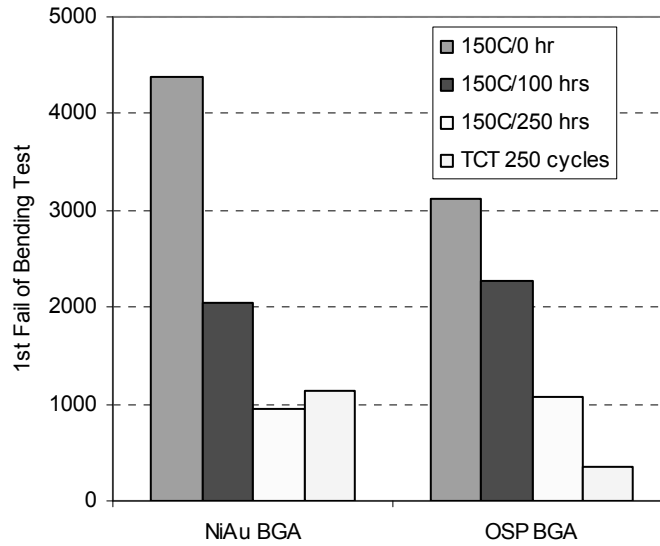


Fig. 23 Effect of TFBGA surface finish on first failure of CBT for BGA on PCB (OSP) for SACM.

For C-Life, a trend can be recognized: ImAg > OSP > ENIG. For first failure, ENIG appears to be more noticeably poorer than the other two finishes.

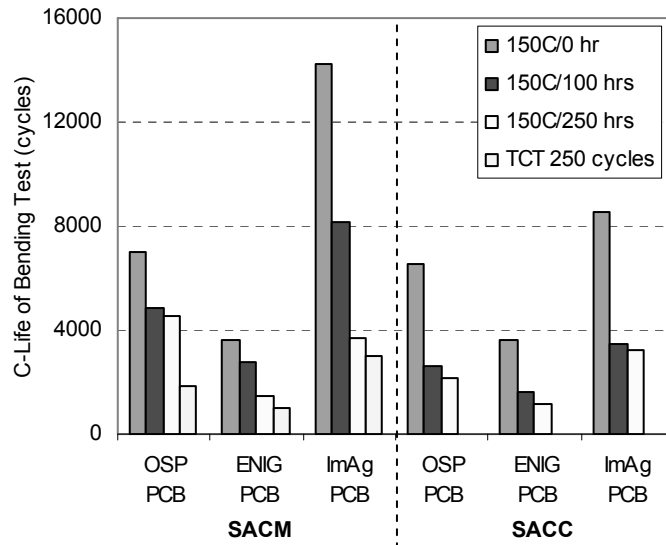


Fig. 24 Effect of PCB surface finish on C-Life of CBT for SACM and SACC for devices assembled with TFBGA (NiAu).

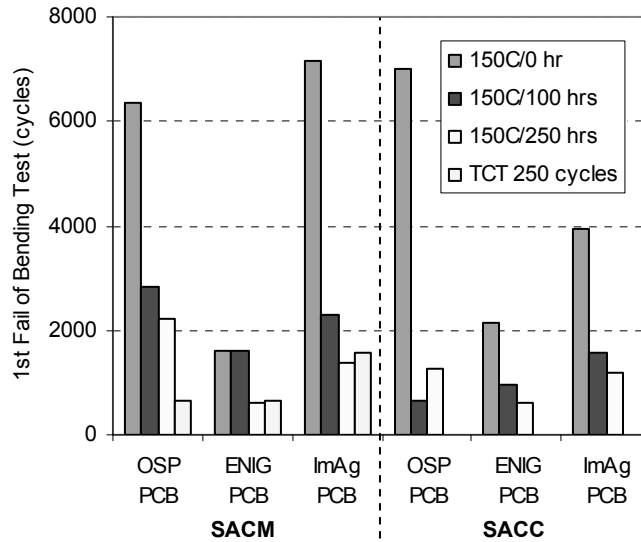


Fig. 25 Effect of PCB surface finish on first failure of CBT for SACM and SACC for devices assembled with TFBGA (NiAu).

The Weibull data, β , η , and ρ , for JDT, TCT, and CBT for most of the systems are listed in Appendix 1.

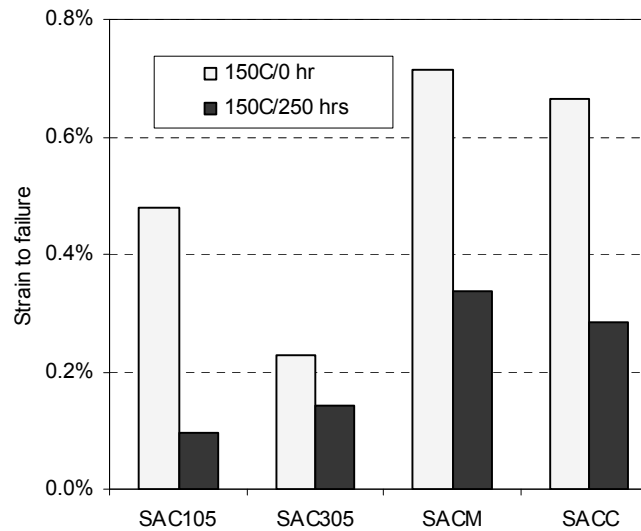


Fig. 26 DBT performance for TFBGA (NiAu) on PCB (OSP).

4. Dynamic Bending Test (DBT)

For devices with TFBGA (NiAu) assembled on PCB (OSP), the DBT performance of various sphere alloys is shown in Fig. 26. The reliability for as reflowed devices can be ranked in the following order:

SACM > SACC > SAC105 > SAC305

However, for thermally aged (150°C/250 hrs) devices, the performance gap between doped SAC105 systems and regular SAC105 increases, and the ranking of alloys altered, as shown below.

SACM > SACC > SAC305 > SAC105

5. Microstructure

Fig. 27 shows the microstructure of interface of solder joints of TFBGA (NiAu) on PCB (OSP) aged at 150°C. SACM and SACC displayed a thinner and smoother interfacial IMC layer than SAC105 at both package side and PCB side. SAC105 also exhibited a bulk solder dispersed with more coarse IMC particles than SACM and SACC.

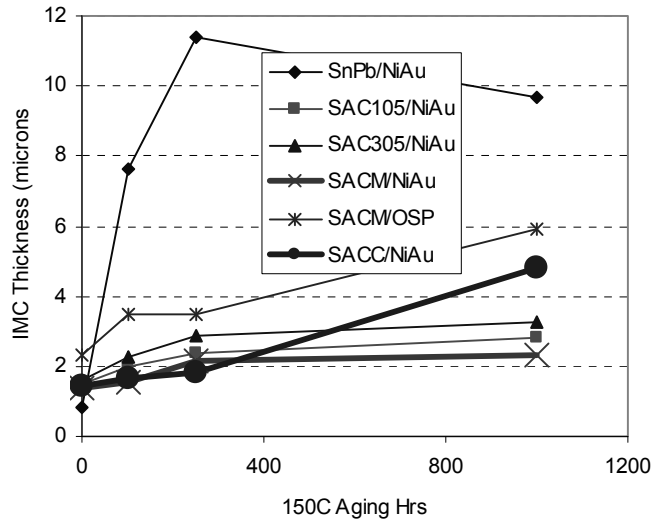


Fig. 28 IMC thickness of TFBGA joints at packaging side mounted on PCB (OSP).

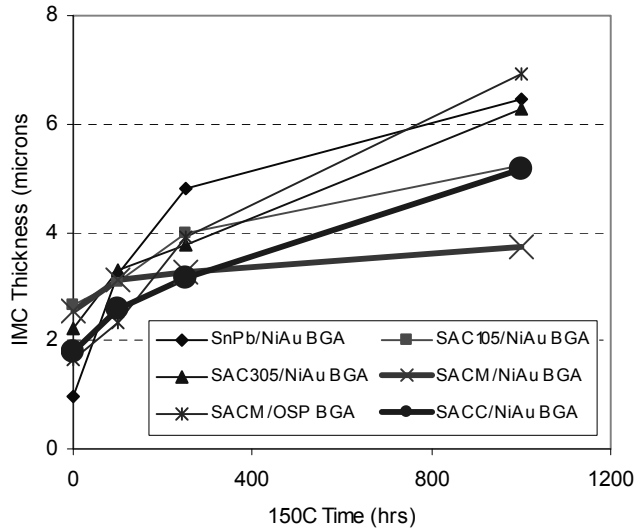


Fig. 29 IMC thickness of TFBGA solder joints at PCB (OSP) side.

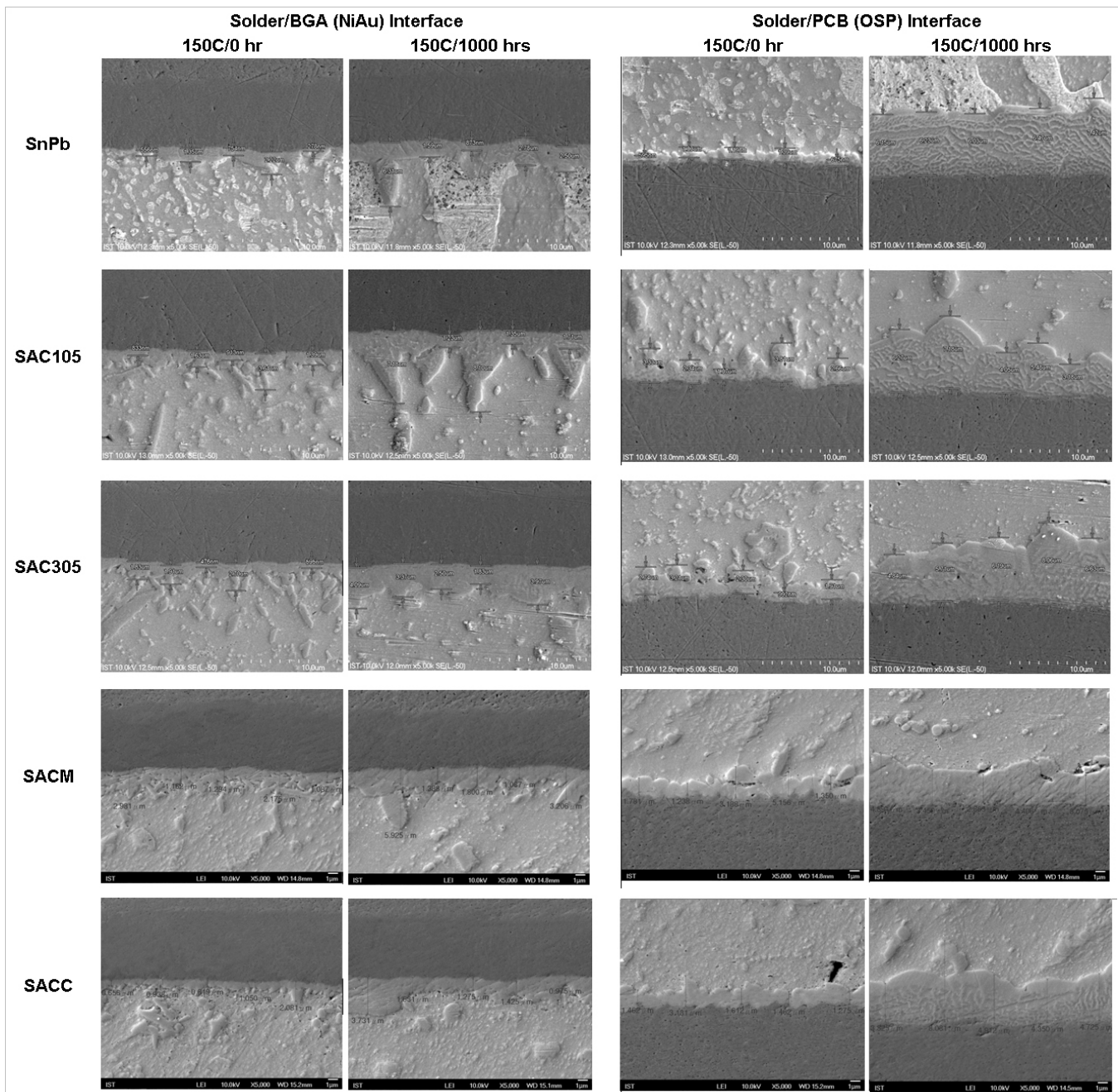


Fig. 27 Interface of solder joints of TFBGA (NiAu) on PCB (OSP) aged at 150°C.

Fig. 28 shows IMC thickness of BGA joints at packaging side (average of 3 balls) mounted on PCB (OSP). Among all, SACM on NiAu had the lowest IMC thickness. On the other hand, OSP showed a faster IMC growth rate than NiAu. This is consistent with other findings [5,6]. It is interesting to note that SACC on NiAu showed a thinner IMC but a similar growth rate as SACM on OSP.

The IMC thickness at PCB (OSP) side is shown in Fig. 29. Again, SACM exhibited the lowest IMC thickness among all, if the packaging side was NiAu. SACC showed a lower thickness than the rest systems, although the IMC growth rate was comparable.

The interfacial IMC morphology is shown in Fig. 30 for solder/TFBGA (NiAu) interface for solder bumps aged at 150°C for various period of time. The solder has been selectively removed by etching, and the IMC at interface is exposed. For SAC105 and SAC305, the IMC rods grew thicker and longer considerably upon aging. SACM had slightly finer IMC particles than SAC alloys in the as reflowed joints. Those IMC particles thickened slower than both SAC alloys upon thermal aging. SACC showed similar behavior as SACM.

Fig. 31 shows the effect of alloy type and thermal aging pretreatment prior to TCT on the microstructure of thermal cycled devices. The optical micrographs indicate the IMC particles of SAC105 coarsened significantly by 150°C/250 hrs thermal aging prior to TCT. The IMC particle size and distribution of SACC without thermal aging are similar to SAC105. For SACM samples without thermal aging pretreatment, the IMC particles are much finer than SAC105, as can be seen in the close up look pictures in Fig. 32. Both SACC and SACM showed no coarsening of the IMC particles with thermal aging pretreatment.

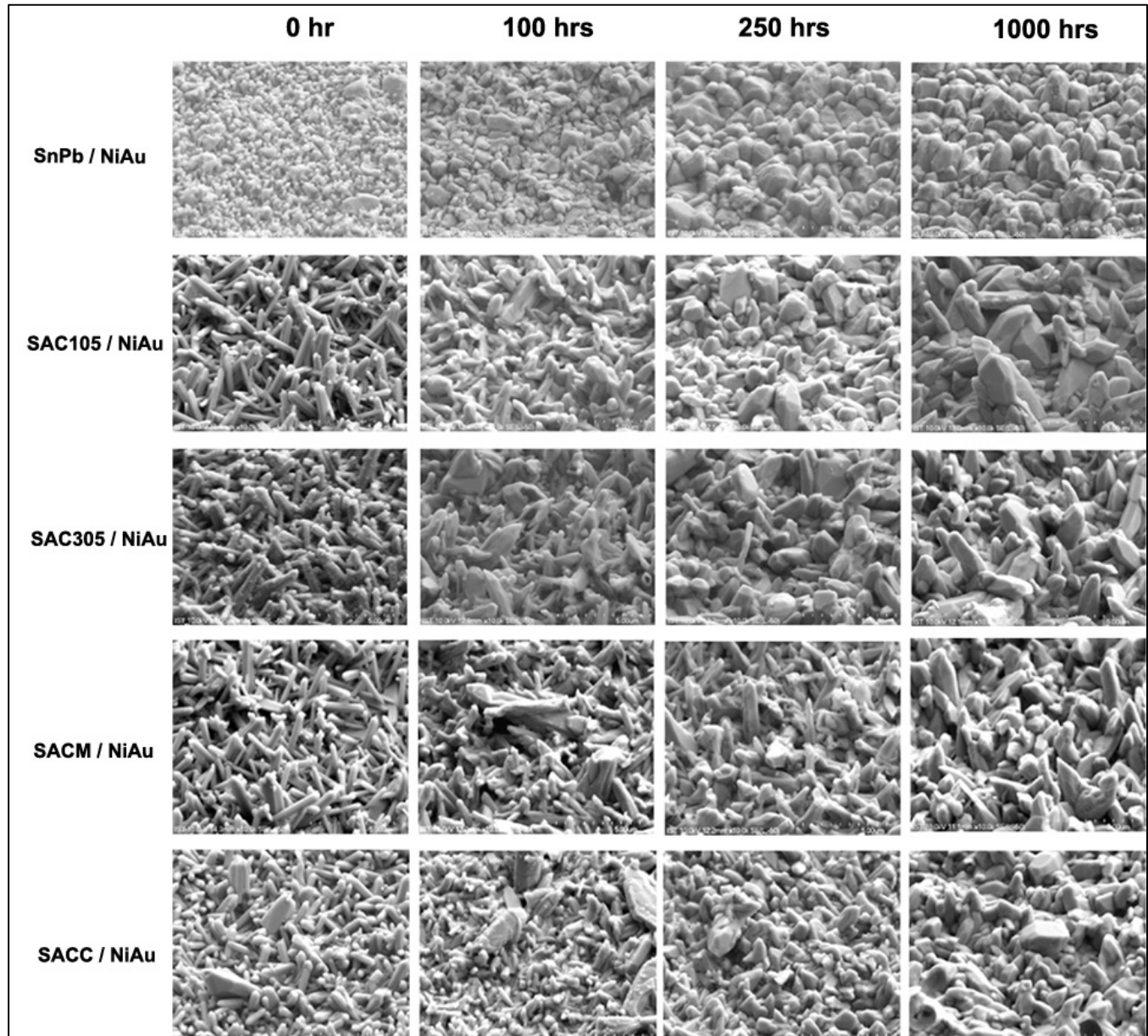
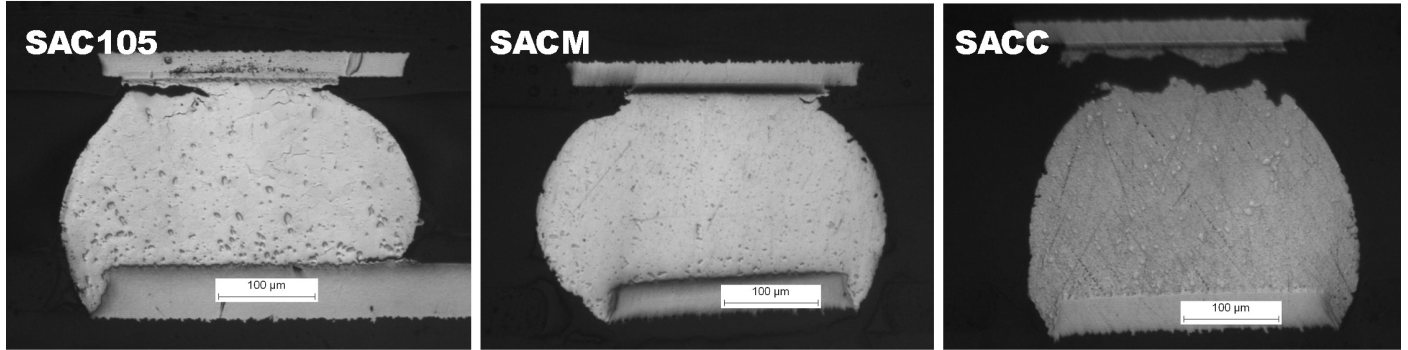
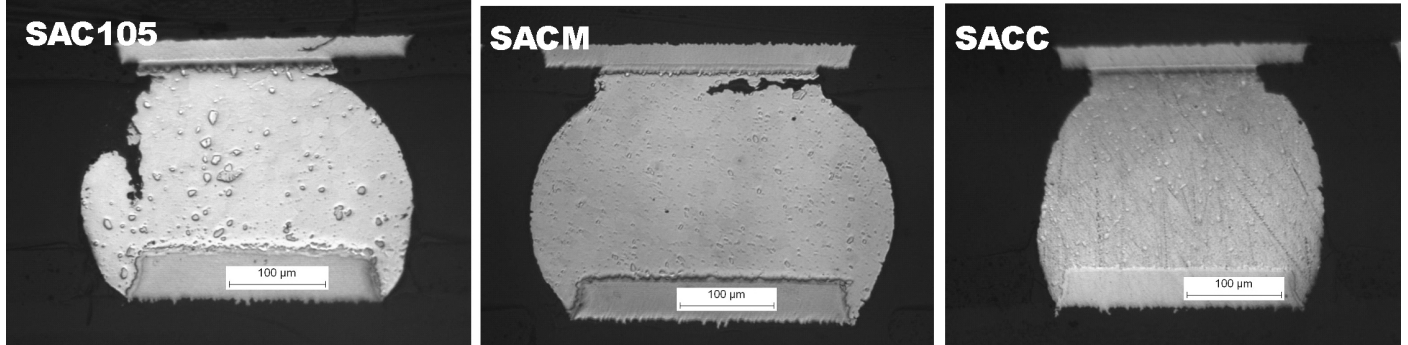


Fig. 30 Intermetallic compounds at solder/TFBGA (NiAu) interface for solder bumps aged at 150°C (10,000X). Solder has been selectively removed by etching.

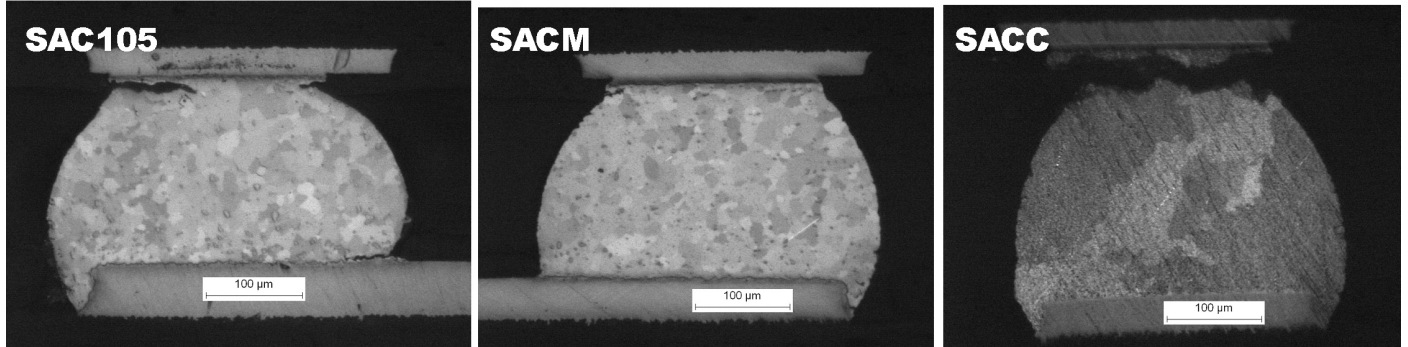
Optical micrographs of solder joints after TCT



Optical micrographs of solder joints preconditioned at 150°C/250 hrs, followed with TCT



Polarized light micrographs of solder joints after TCT



Polarized light micrographs of solder joints preconditioned at 150°C/250 hrs, followed with TCT

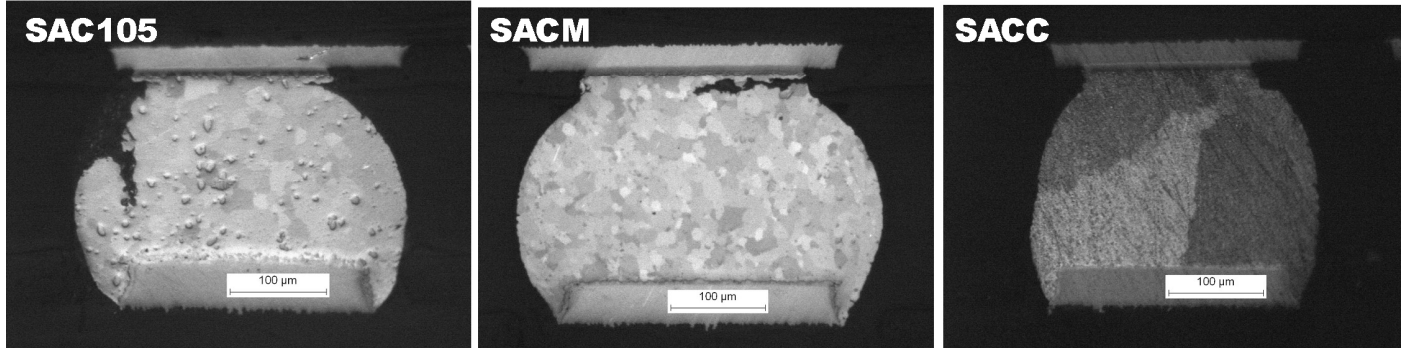


Fig. 31 Effect of alloy type and thermal aging pretreatment prior to TCT on the microstructure of thermal cycled

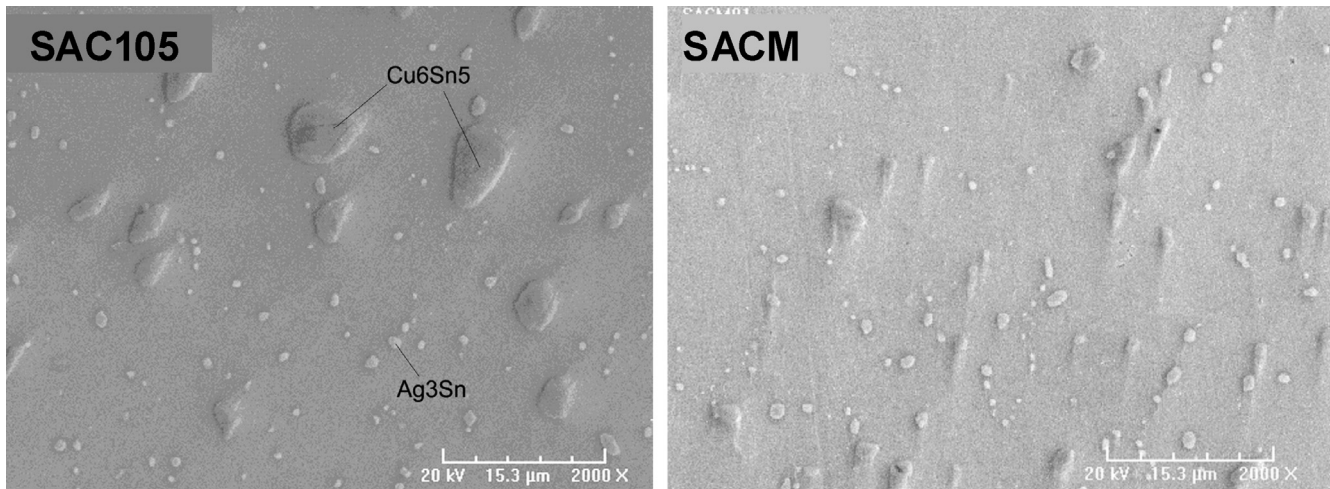


Fig. 32 Microstructure of solder joints of TFBGA (NiAu) on PCB (OSP) after TCT.

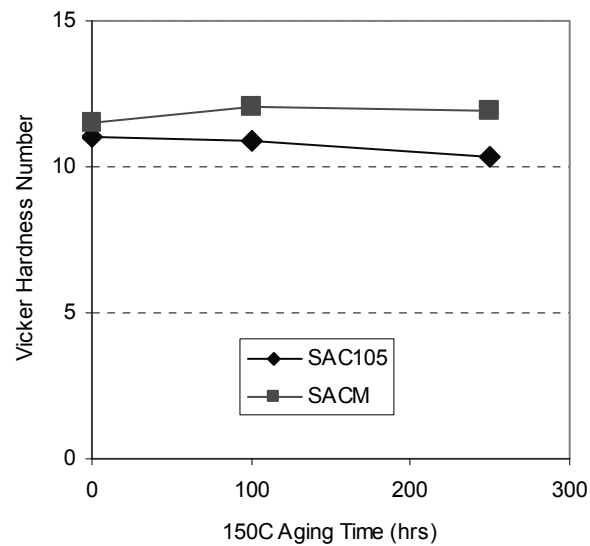


Fig. 33 Effect of 150°C aging time prior to TCT on HV for solder joints of TFBGA (NiAu) on PCB (OSP) after TCT.

In Fig. 31, the polarized light micrographs (PLM) indicate SAC105 had similar multiple grain structures as SACM for samples without thermal aging pretreatment. With thermal aging pretreatment, the number of grains of SAC105 degenerated into a reduced number, while that of SACM maintained the same. For SACC, only very few grains can be discerned for samples without thermal aging pretreatment. The low grain number feature was maintained with additional thermal aging pretreatment.

6. Mechanical Properties

The hardness of solder joints after TCT was determined, as shown in Fig. 33. Thermal aging prior to TCT caused the hardness of SAC105 joints to decrease. On the other hand, SACM was insensitive to this thermal aging pretreatment, and maintained the same hardness as the sample without thermal aging.

The tensile properties of several lead-free alloys were measured, as shown in Fig. 34. SAC305 exhibited the highest value in tensile strength, yield strength, Young's modulus, and elongation (%). SACM and SAC105 are fairly comparable, except that SACM is better than SAC105 in elongation.

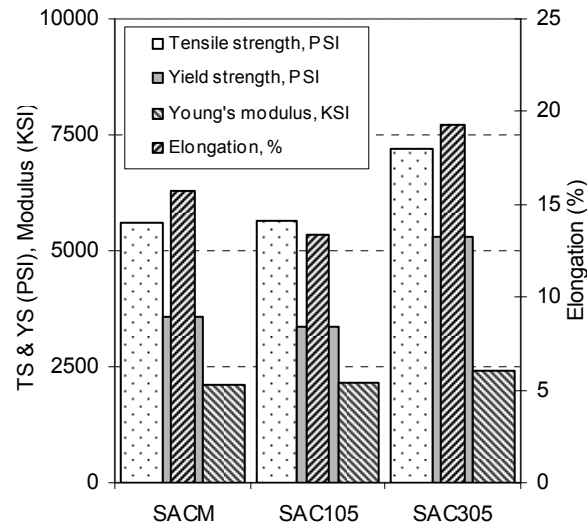


Fig. 34 Mechanical properties of SACM, SAC105, and SAC305.

Discussion

1. TCT Performance

SACM and SACC showed a higher TCT reliability than that of SAC105. Both also compared favorably with SAC305, as shown in Fig. 12, 13, and 14. The high TCT reliability of SACM and SACC can be attributed to their high stability in microstructure, as shown in Fig. 31 and Fig. 32. Presence of Mn or Ce effectively suppressed the coarsening of IMC particles, thus maintained the hardness of solder joint. On the other hand, SAC105 displayed coarsening of IMC particles, and the resultant decrease in hardness of solder joints with increasing thermal aging, as shown in Fig. 33.

The greater TCT reliability may also be attributed to (1) finer IMC texture at interface, and (2) thinner IMC layer. It has been reported that Co, Ni or Pt inclusion in 97Sn3Ag soldered onto Cu substrate did not coarsen IMC scallop size or increase IMC thickness and grain size significantly after 4 times solder reflow. This IMC suppression phenomenon was accomplished by having Co, Ni and Pt dissolved in IMC layer [7]. The grain size stability can be attributed to the pinning of grain boundary by the abundant fine IMC particles. In view of this, it is reasonable to speculate that the IMC suppression phenomenon observed in SACM and SACC was also resulted from inclusion of Mn or Ce in the IMC.

The coarsening of IMC particles should be responsible for the grain coarsening of SAC105, as shown in the polarized light micrographs in Fig. 31. Solder with coarsened grains in general tends to exhibit a higher creep rate [8] and consequently a poorer thermal fatigue life. In contrast, SACM showed no sign of grain coarsening. This phenomenon is consistent with the IMC and grain size suppression effect observed for Co, Ni and Pt.

However, the role of a fine grain structure in high TCT reliability should not be over emphasized. In Fig. 31, SACC showed a steady but coarse grain structure. And, as stated above, SACC joints are fairly high in TCT reliability. Thus, it can be concluded that a stable and fine IMC structure is the primary contributing factor, and a stable grain structure is the secondary cause for SACM and SACC to exhibit a high TCT reliability.

2. Drop Test Performance

Both JDT and DBT are tests designed to predict the resistance against drop failure for portable devices. By examining Fig 6, 7, and 26, the results of both methods indicate that SACM and SACC performed considerably better than SAC105 and SAC305. By examining Fig. 27-32, both SACM and SACC exhibit finer IMC structure at interface. Besides, SACM exhibits a thinner IMC layer, which has also been reported in previous studies [9, 10]. SACC showed a thinner IMC layer at PCB side.

Addition of small amount of certain additives not only suppresses the IMC growth and grain coarsening, but also causes low frequency of occurrence of IMC fracture in high impact pull test, and was very effective for improving drop test performance [7]. Presumably inclusion of these additives in the IMC layer reduced the brittleness of IMC structure. The findings in those studies help explaining the improved drop test performance of SACM and SACC.

3. CBT Performance

In CBT test, the reliability ranking was observed as: SAC305 >> SACC, SACM, SAC105 > SnPb. The superior performance of SAC305 can be attributed to its mechanical property, as shown in Fig. 34.

Since all lead-free alloys showed a higher CBT reliability than the control SnPb, the relative performance of lead-free systems is considered non-consequential in terms of finding a valid lead-free alternative for SnPb.

4. Surface Finish

The relative performance of PCB surface finishes in the three tests JDT, TCT, and CBT is interestingly consistent: ImAg > OSP > ENIG.

On the other hand, the relative performance of TFBGA surface finishes is more complicated. In TCT, NiAu > OSP. In CBT, NiAu > OSP for as reflowed or thermally cycled samples. In JDT, for thermally cycled devices, NiAu > OSP. For as reflowed devices or thermally aged devices, OSP > NiAu.

All these results indicate that for thermally cycled devices the drop, cyclic bending and thermo-mechanical fatigue reliabilities with NiAu finished packages are higher than those with OSP finished packages. The reason for these may be due to the fact that the solder joints with asymmetric substrates (Cu:NiAu) have lower creep rates than those with symmetric substrates (Cu:Cu) [11]. In view of these reliability results in the present paper, NiAu should be a preferred surface finish for BGA packages if assembled in the popular OSP finished PCBs since all electronic devices experience temperature cycling in service.

Conclusion

The Mn or Ce doped low cost SAC105 alloys achieved a higher drop test and dynamic bending test reliability than SAC105 and SAC305, and exceeded SnPb for some test conditions. More significantly, being a slightly doped SAC105, both SACM and SACC matched SAC305 in thermal cycling performance. In other words, the low cost SACM and SACC achieved a better drop test performance than the low Ag SAC alloys plus the desired thermal cycling reliability of high Ag SAC alloys. The mechanism for high drop performance and high thermal cycling reliability can be attributed to a stabilized microstructure, with uniform distribution of fine IMC particles, presumably through the inclusion of Mn or Ce in the IMC. The cyclic bending results showed SAC305 being the best, and all lead-free alloys are equal or superior to SnPb. The reliability test results also show that NiAu is a preferred surface finish for BGA packages over OSP if assembled in the popular OSP finished PCBs.

Reference

1. Lee, Y.J., Crosbie, P., Brown, M. and Zbrzezny, A., "Reliability of Wafer Level Chip Scale Packages (WL-CSP) under Dynamic Loadings", IEEE ECTC, 2008, pp.1782-1786, Lake Buena Vista, Florida, 2008.
2. Lal, A., Bradley, E., and Sharda, J., " Effect of Reflow Profiles on the Board Level Drop Reliability of Pb-free (SnAgCu) BGA Assemblies ", IEEE ECTC 2005.
3. Reiff, D. and Bradley, E., "A Novel Mechanical Shock Test Method to Evaluate Lead-free BGA Solder Joint Reliability", IEEE ECTC 2005.
4. Lim, C.T., Lim C.T., Ang C.W., Tan L.B., Seah S.K.W., Wong E.H., "Drop Impact Survey of Portable Electronic Products" IEEE ECTC, 2003, pp. 113-120.
5. Kao, C. R., "Cross-interaction between Cu and Ni in lead-free solder joints", TMS Lead Free Workshop, San Antonio, TX, March 12, 2006.
6. Song, F. and Lee, S. W. R., "Investigation of IMC Thickness Effect on the Lead-free Solder Ball Attachment Strength: Comparison between Ball Shear Test and Cold Bump Pull Test Results", 56th ECTC Proceedings, P. 1196-1203, San Diego, CA, May 30-June 2, 2006.
7. Amagai, M., " A Study of Nano Particles in SnAg-Based Lead Free Solders for Intermetallic Compounds and Drop Test Performance", 56th ECTC Proceedings, P. 1170-1190, San Diego, CA, May 30-June 2, 2006
8. Joo, D. K. and Yu, J., "Effects of Microstructure on the Creep Properties of the Lead-free Sn-3.5Ag-Cu Solders", 52nd ECTC, S29-P5, San Diego, CA, May 28-31, 2002.
9. Liu, W.P. and Lee, N.-C., "Novel SACX Solders with Superior Drop Test Performance", SMTA International, Chicago, IL, September, 2006.
10. Liu, W.P. and Lee, N.-C., "The Superior Drop Test Performance of SAC-Ti Solders and Its Mechanism", 58th ECTC, Lake Buena Vista, Florida, May 27-30, 2008.
11. Lee, Kyu-Oh, Morris, J.W., Hua, F., "Substrate effects on the creep properties of pure Sn solder joints", Proceedings International Symposium on Advanced Packaging Materials: Processes, Properties and Interfaces. March 16-18, 2005, P. 17 – 20.

Appendix 1 Weibull data for JDT, TCT, and CBT.

JEDEC Drop Test Weibull Plot Data												
Alloy	150C/0 hr			150C/100 hrs			150C/250 hrs			250 TCT		
	β	η	ρ	β	η	ρ	β	η	ρ	β	η	ρ
SnPb	3.144	111	0.981	2.458	79.72	0.893	2.915	108.8	0.99	3.583	139.7	0.964
SAC105	1.429	197.3	0.972	1.079	61.76	0.919	1.002	34.24	0.95	1.345	120.9	0.952
SAC305	1.139	31.85	0.987	0.953	47.52	0.965	1.249	27.42	0.957	1.063	58.84	0.926
SACM	2.273	237.2	0.962	1.509	92.59	0.96	1.047	69.54	0.929	2.177	179.2	0.974
SACC	3.873	239.4	0.969	1.055	199.6	0.953	1.08	114.3	0.969	1.254	202.1	0.971
Thermal Cycle Test Weibull Plot Data												
Alloy	150C/0 hr			150C/100 hrs			150C/250 hrs					
	β	η	ρ	β	η	ρ	β	η	ρ	β	η	ρ
SnPb	8.667	1305	0.967	7.743	1125	0.938	7.058	1112	0.944			
SAC105	3.409	1541	0.981	7.646	1388	0.941	7.943	1468	0.963			
SAC305	7.506	2154	0.968	8.35	1861	0.996	5.805	1906	0.965			
SACM	3.169	1706	0.974	7.22	1762	0.982	5.780	2034	0.946			
SACC	5.161	1809	0.898	5.66	1896	0.929	6.845	2385	0.966			
Cyclic Bending Test Weibull Plot Data												
Alloy	150C/0 hr			150C/100 hrs			150C/250 hrs			250 TCT		
	β	η	ρ	β	η	ρ	β	η	ρ	β	η	ρ
SnPb	3.077	4046	0.923	4.615	2940	0.979	3.452	2854	0.93	2.282	8610	0.927
SAC105	3.683	8592	0.973	5.032	4266	0.979	4.667	2991	0.988	3.936	3723	0.934
SAC305	1.67	65302	0.952	2.934	9811	0.987	3.042	6913	0.986	3.596	10367	0.979
SACM	3.426	9018	0.991	3.657	3807	0.973	3.326	1953	0.952	3.079	2190	0.96
SACC	3.038	8634	0.975	2.155	3071	0.96	3.755	2164	0.959	1.481	1589	0.94

Achieving High Reliability Low Cost Lead-Free SAC Solder Joints Via Mn Or Ce Doping

Dr. Weiping Liu¹, Dr. Ning-Cheng Lee¹, Adriana Porras², Dr. Min Ding², Anthony Gallagher³, Austin Huang⁴, Scott Chen⁴, and Jeffrey ChangBing Lee⁵

1 Indium Corporation; 2 Freescale Semiconductor
3 Motorola Inc; 4 Advanced Semiconductor Engineering Group;
5 IST-Integrated Service Technology Inc

Introduction

- SAC with high Ag good in thermal fatigue performance, but poor in drop test performance
- SAC with low Ag OK in drop test, but poor in thermal fatigue performance
- A Pb-free alloy with improved drop test performance, and good in thermal fatigue performance badly needed.
- **SAC105+Mn or Ce** studied here

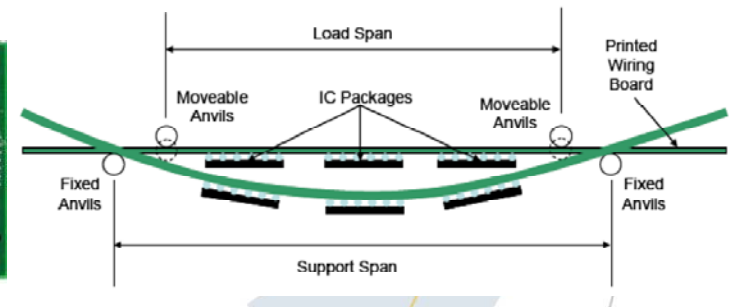
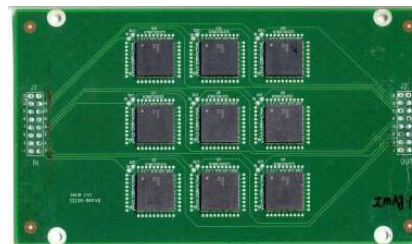
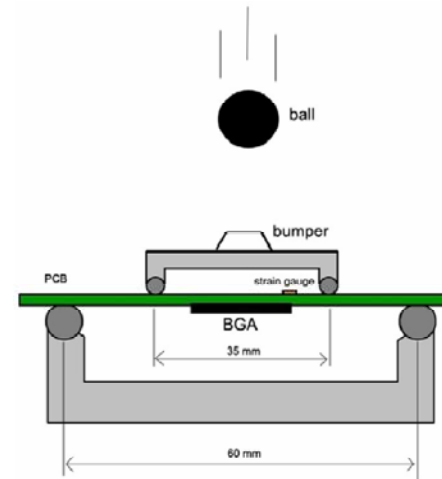
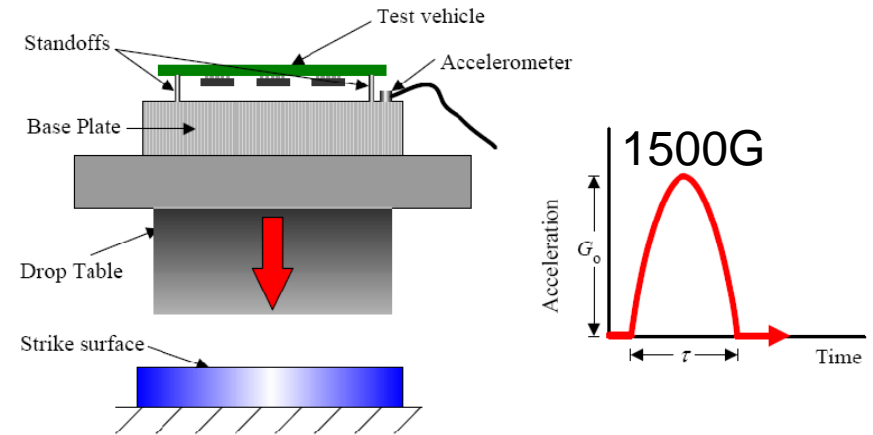
Experimental Design

- New Alloys
 - SAC105+0.05Mn (SACM)
 - SAC105+0.02Ce (SACC)
- DOE for JEDEC drop test & TCT

Package	Daisy TFBGA244 12X12					
Ball/pitch (mm)	0.3/0.5	0.3/0.5	0.3/0.5	0.3/0.5	0.3/0.5	0.3/0.5
Solder ball	SnPb	SAC10 5	SAC30 5	SACM	SACM	SACC
Surface finish of substrate	NiAu	NiAu	NiAu	NiAu	OSP	NiAu
Solder paste	SnPb	SAC30 5	SAC30 5	SAC30 5	SAC30 5	SAC30 5
Reflow profile	220C	245C	245C	245C	245C	245C
PCB	High Tg FR4/8 layer/NVIP/NSMD/OSP (ENIG, ImAg)					

Test Design

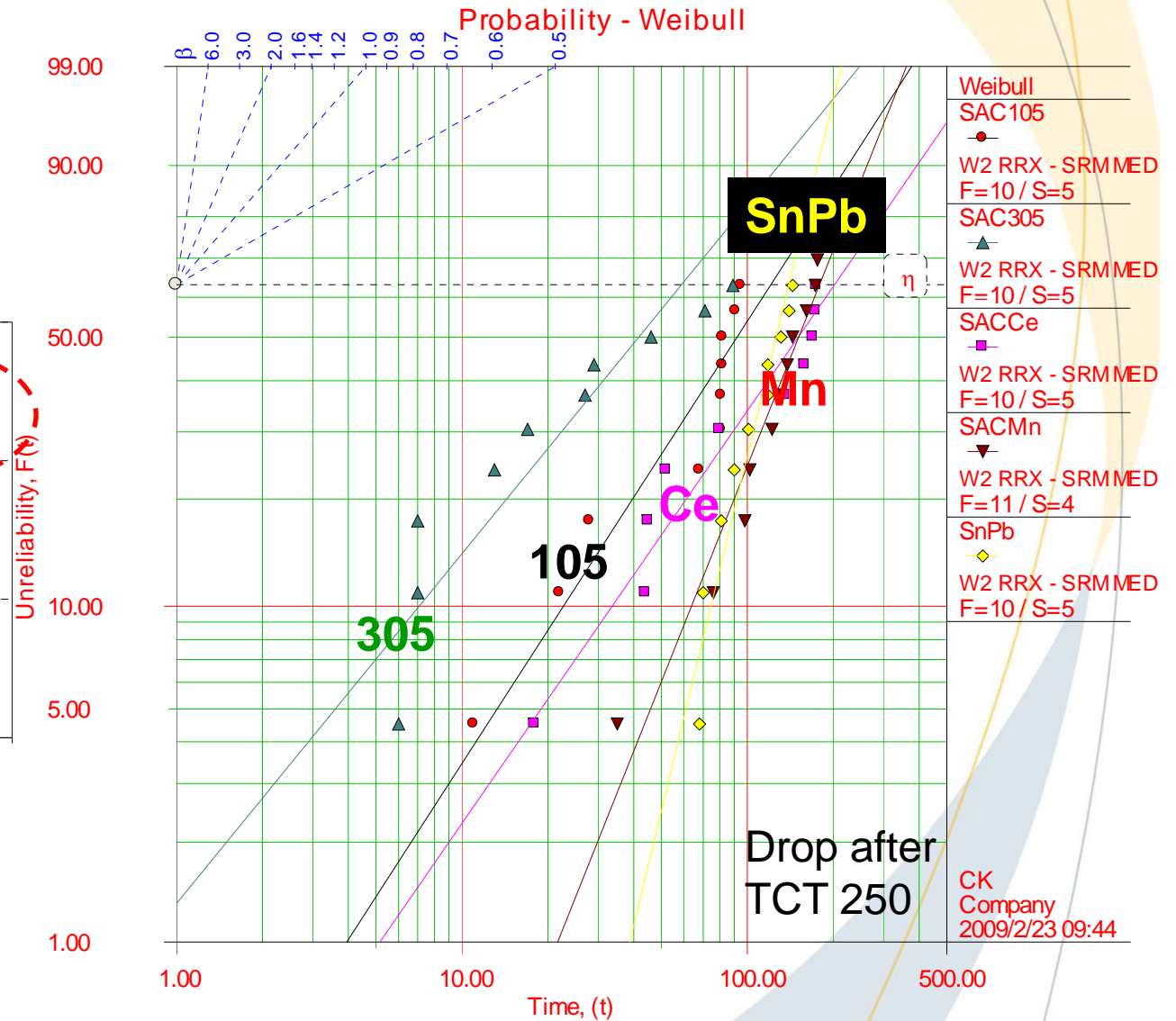
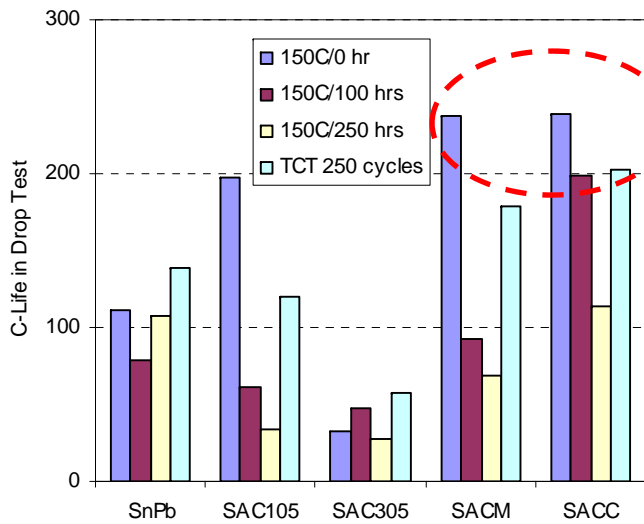
- JEDEC Drop Test (JESD22-B111)
 - Fail when > 1000 ohms
- Dynamic Bending Test
 - Board strain at 1st fail
 - Dye & pry
- Thermal Cycling Test
 - - 40C/125C
 - 42 min/cycle, ramp 11 min, dwell 10 min
 - Fail when > 20% Resistance increase
- Cyclic Bending Test
 - 1 Hz/2mm
 - Paste SAC387
 - Fail when > 1000 ohms



JEDEC Drop Test Results

SACM, SACC ≥ SnPb ≥ 105 > 305

ReliaSoft's Weibull++ 6.0 - www.Weibull.com

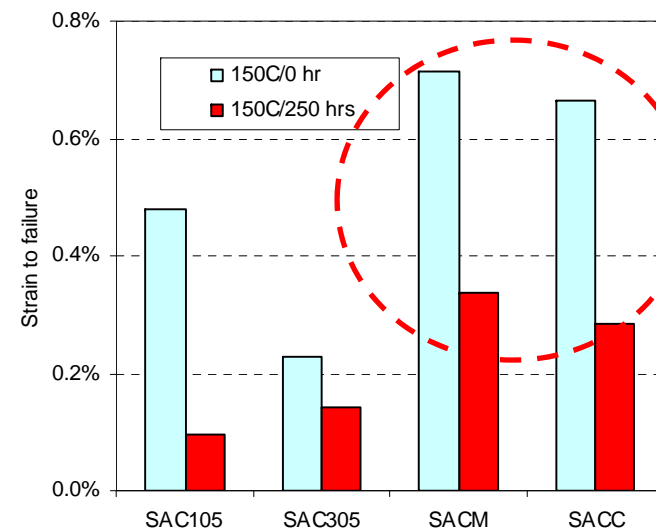
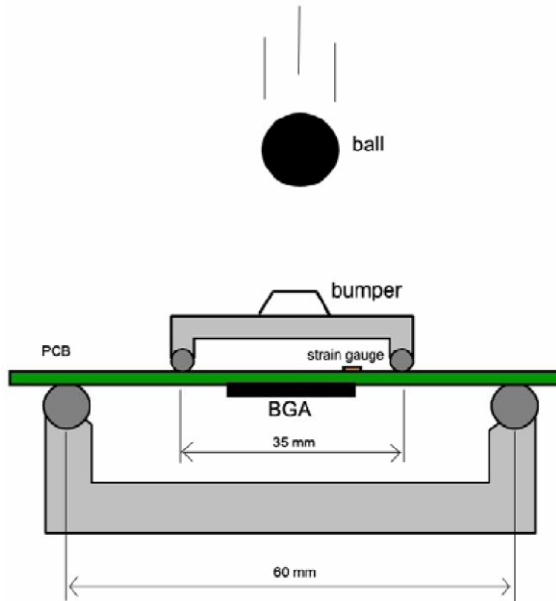


Dynamic Bending Test Result

SACM ≥ SACC > 105 > 305

Failure Criteria: 0.5% strain level		TFBGA (Bravo)			
Package					
ball/pitch (mm)		0.3/0.5	0.3/0.5	0.3/0.5	0.3/0.5
surface finish (substrate)		NiAu	NiAu	NiAu	NiAu
solder ball		SAC105	SAC305	SAC105Mn	SAC105Ce
Solder paste		SAC387			
reflow profile		Linear ramp profile, peak 235C			
PCB (FR4/8 layer/NVIP/SMD)		80	80	80	80
Thermal aging 150C/0hr	Failure Criteria(Strain)	0.5049%	0.2406%	0.7490%	0.6963%
Thermal aging 150C/250hr	Failure Criteria(Strain)	0.0999%	0.1493%	0.3550%	0.2968%

*SACM is SAC105 + Mn dopant
SACC is SAC105 + Ce dopant

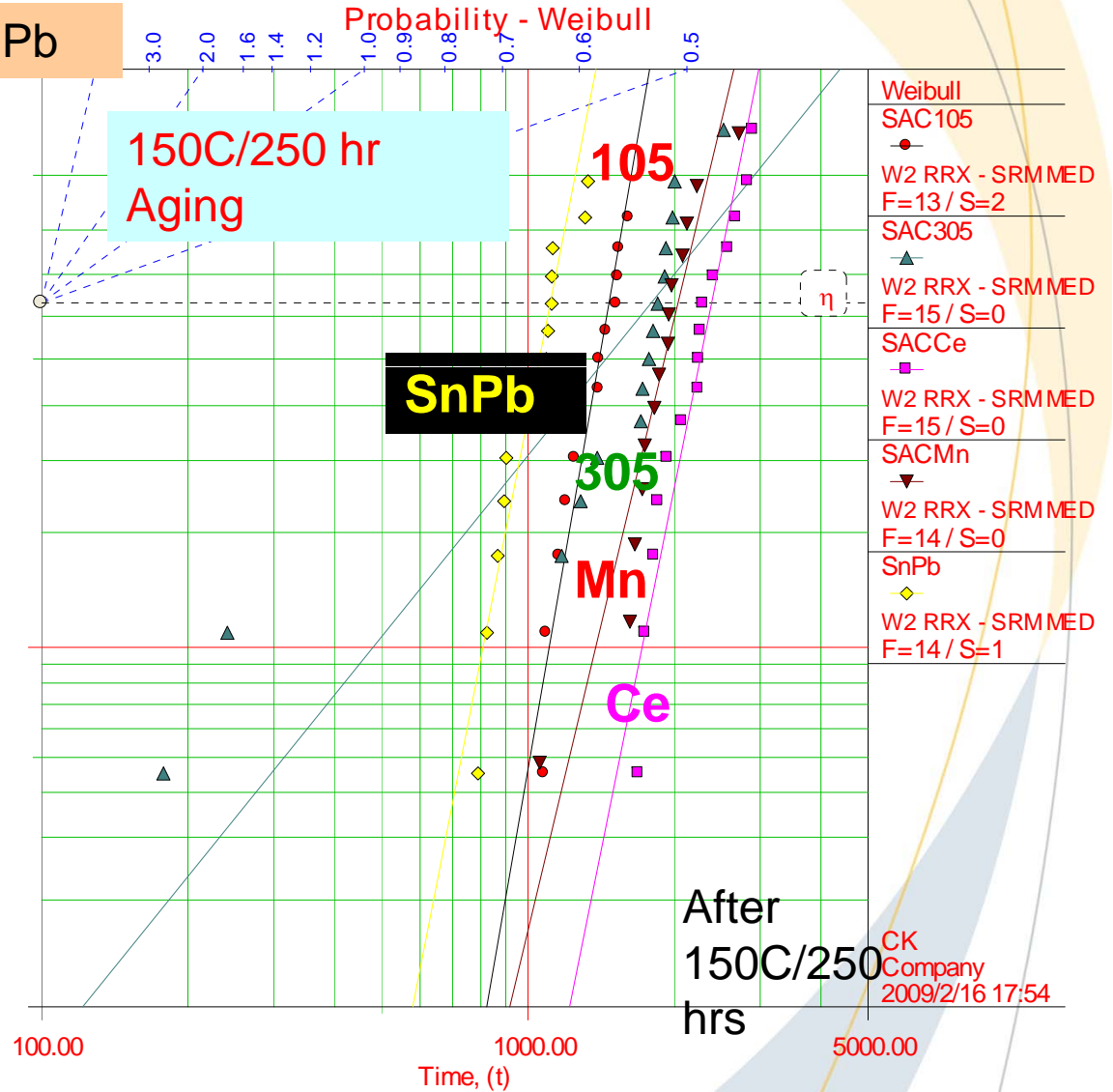
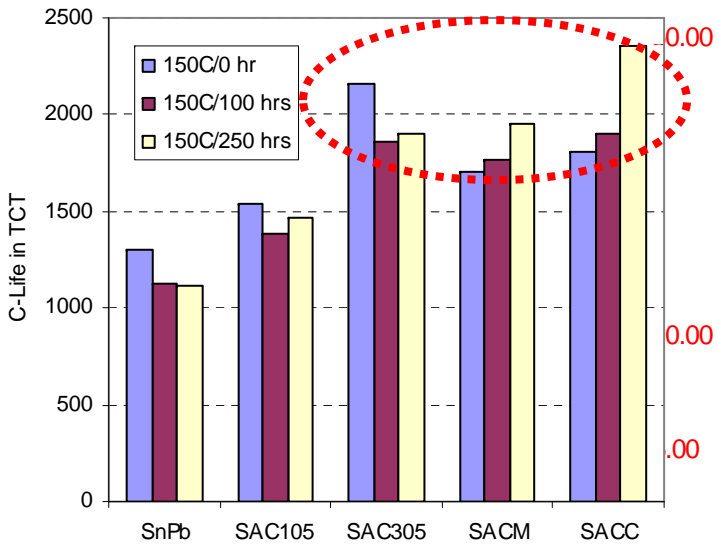




TCT (-40C/125C) Results TFBGA on PCB (OSP)

ReliaSoft's Weibull++ 6.0 - www.Weibull.com

SACC, SACM, 305 > SAC105 > SnPb



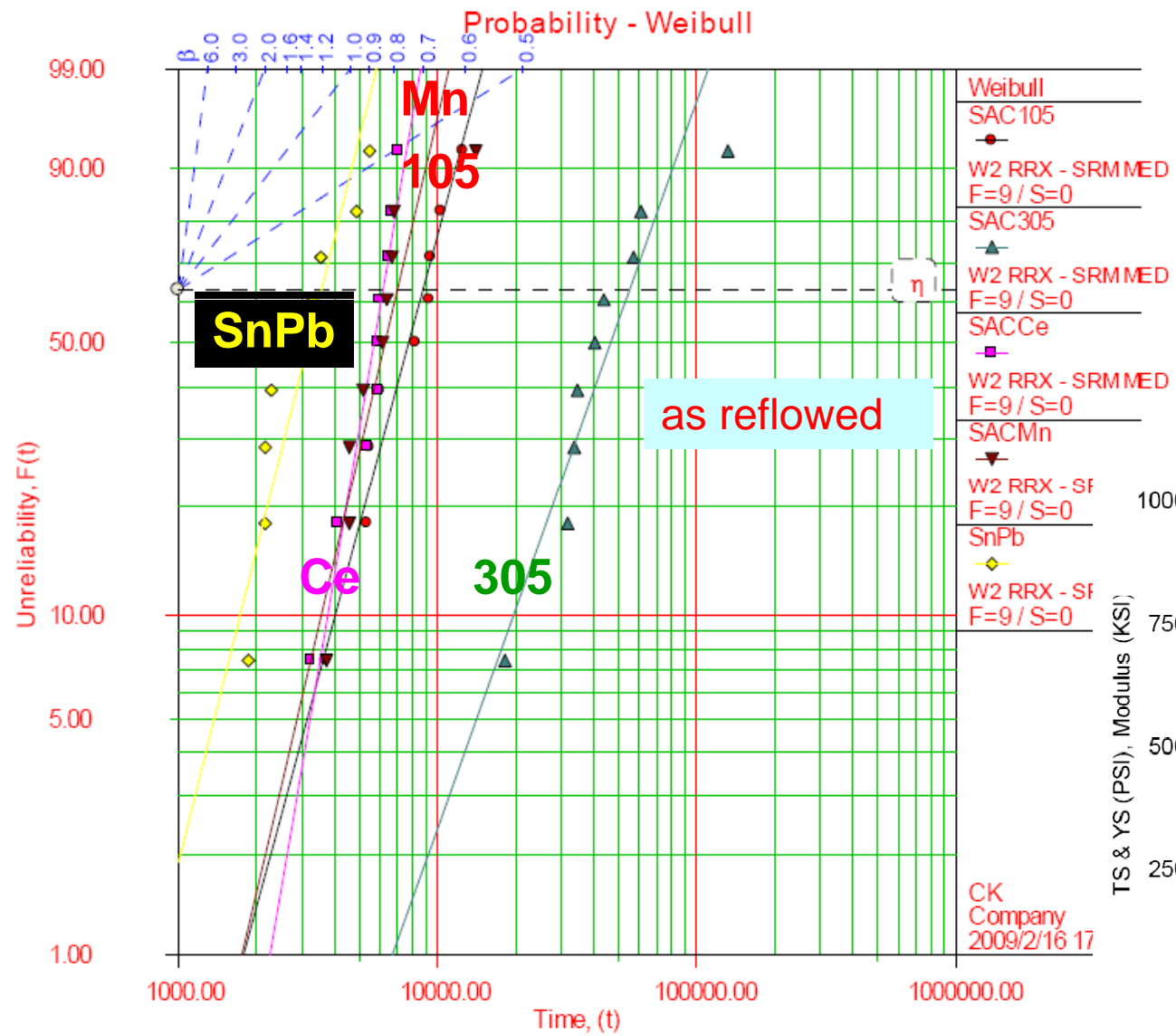


CBT Test Results

TFBGA on

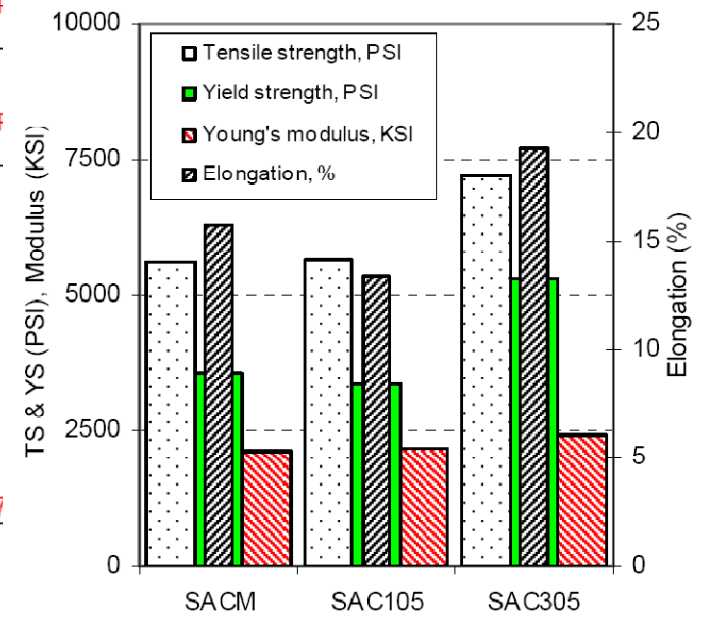
PCB (OSP)

305 > 105, SACM, SACC > SnPb



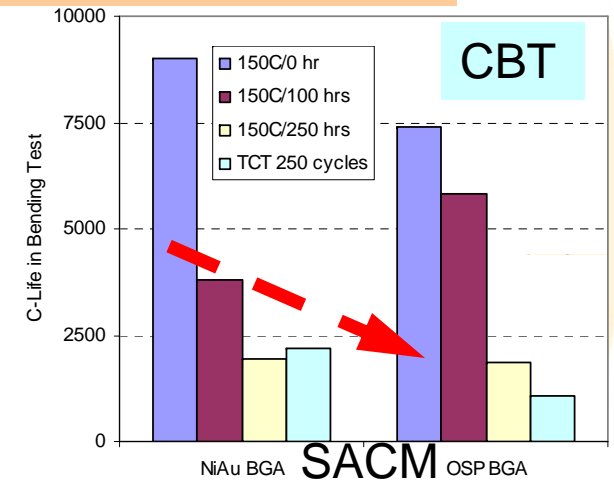
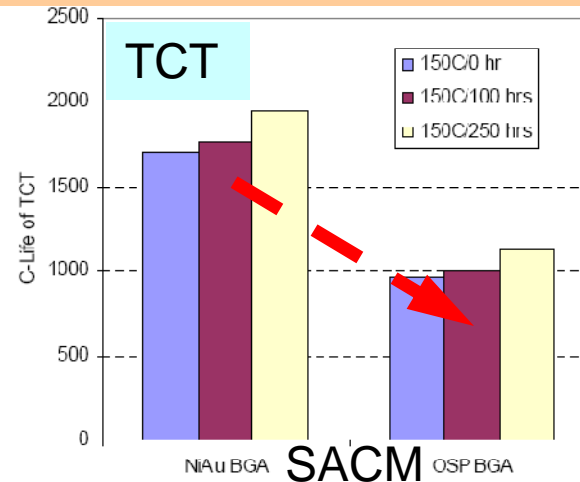
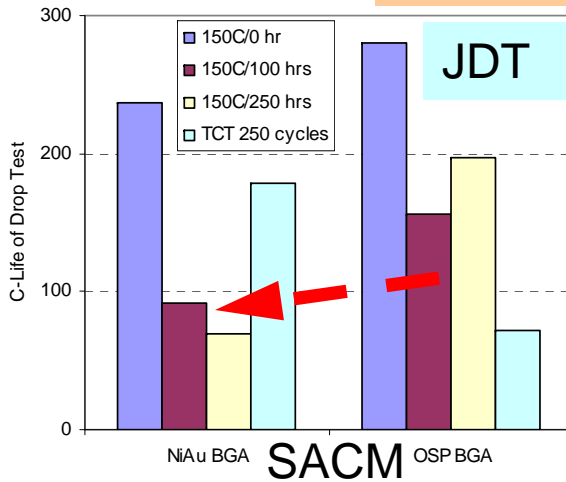
All LF are better than SnPb.

SAC305 exhibited the highest value in TS, YS, Young's modulus, and elongation (%).

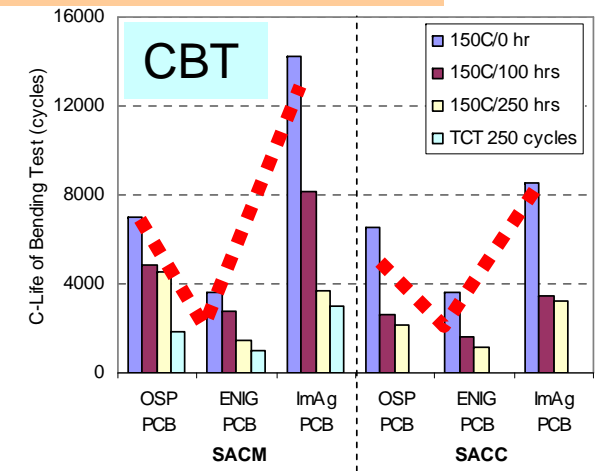
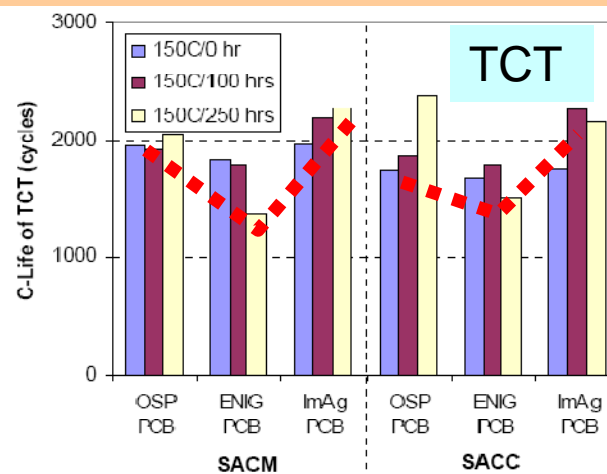
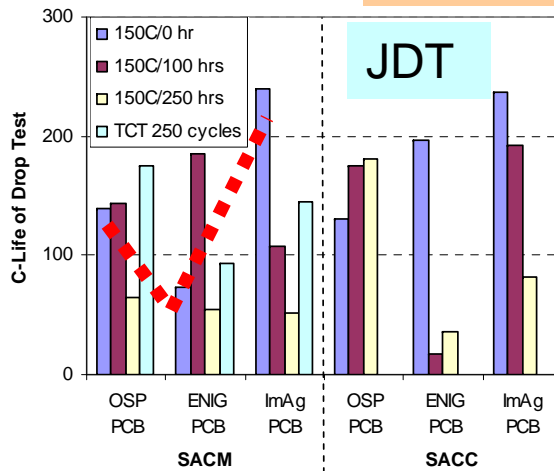


Effect of Surface Finish

Package: NiAu \geq OSP (in general)



PCB: Weak trend ImAg > OSP > ENIG (in general)



Solder/BGA (NiAu) Interface

150C/0 hr

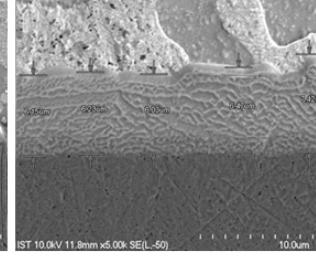
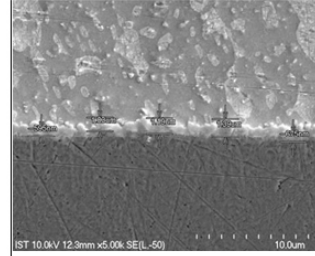
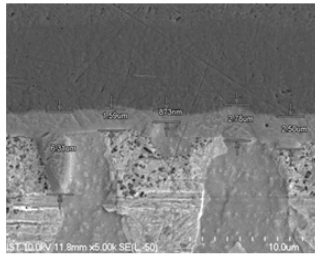
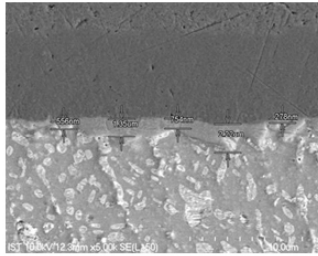
150C/1000 hrs

Solder/PCB (OSP) Interface

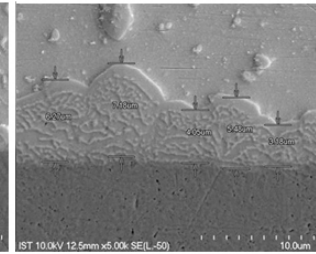
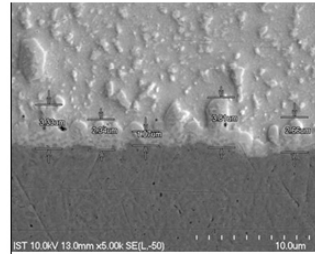
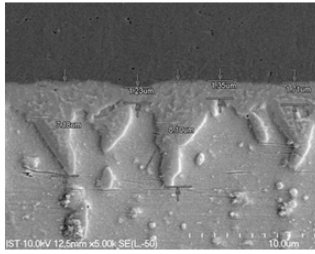
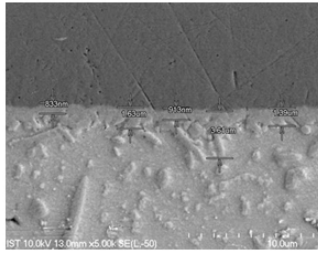
150C/0 hr

150C/1000 hrs

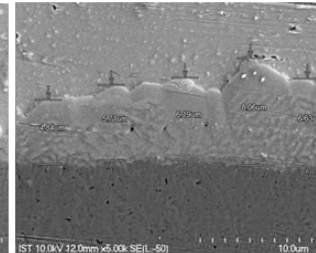
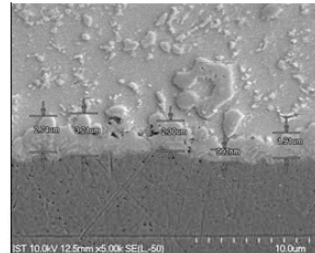
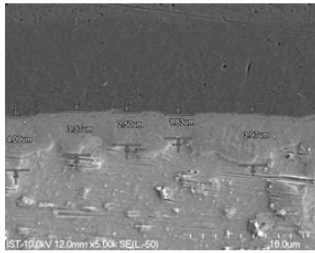
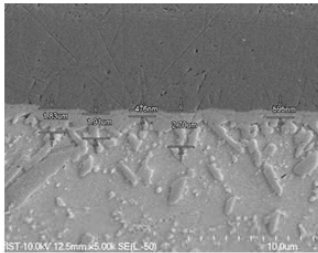
SnPb



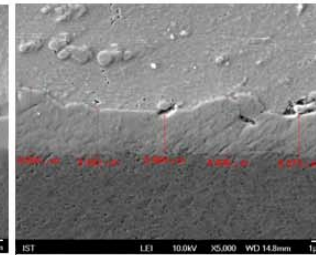
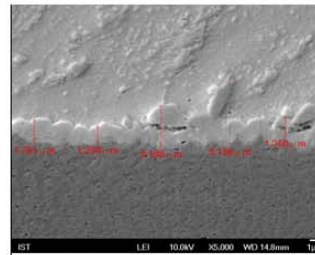
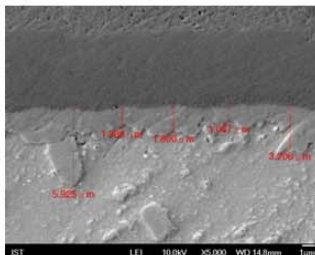
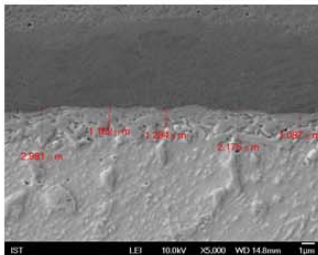
SAC105



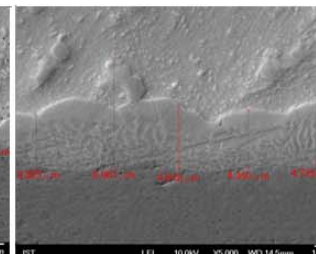
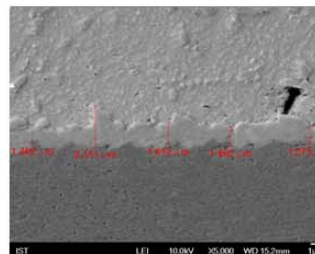
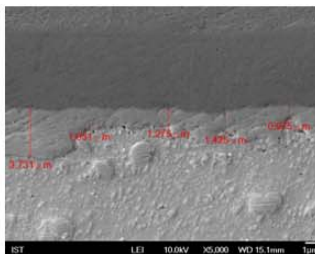
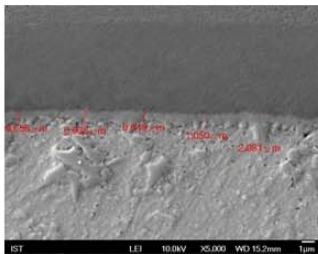
SAC305



SACM



SACC



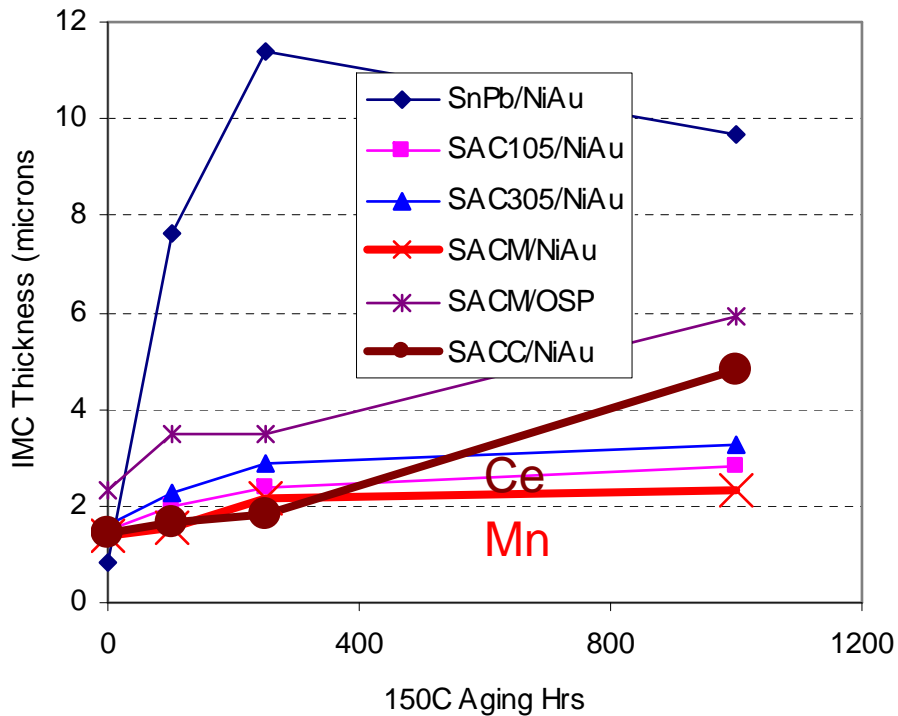
SACM and SACC displayed

(a) thinner and smoother interfacial IMC layers

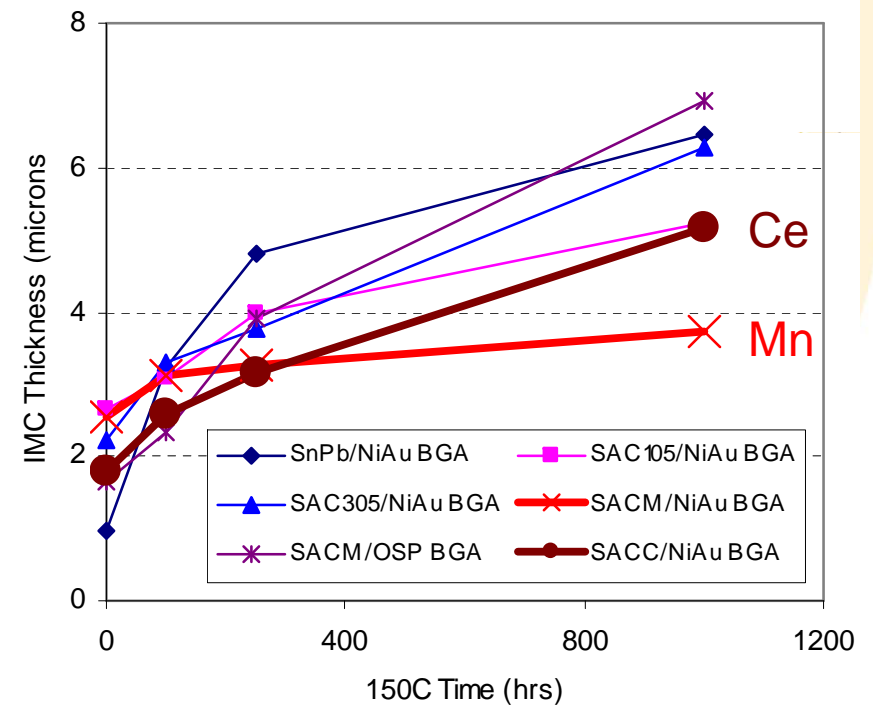
(b) finer IMC particles within bulk solder

Mn & Ce Suppressed IMC Growth

On package side



On PCB side



150C

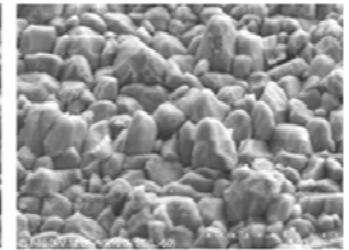
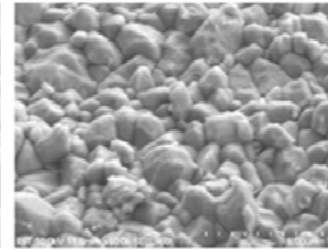
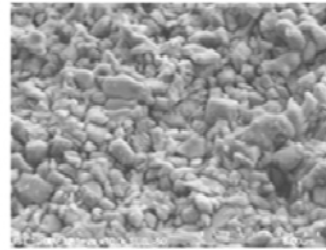
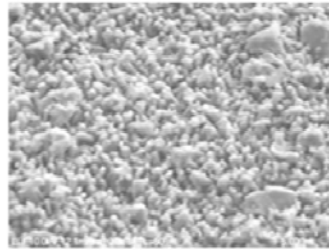
0 hr

100 hrs

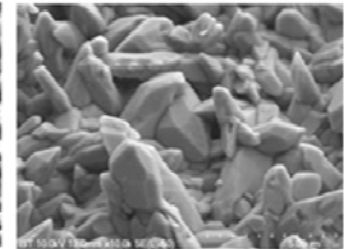
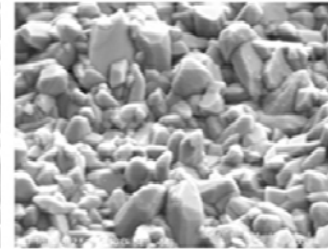
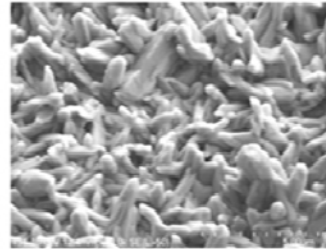
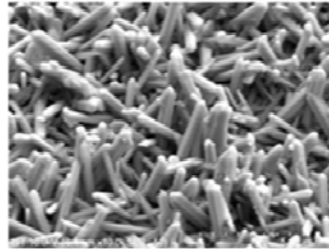
250 hrs

1000 hrs

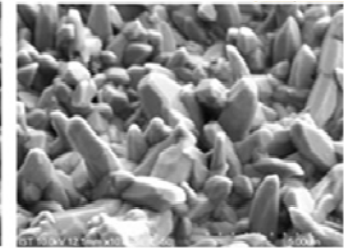
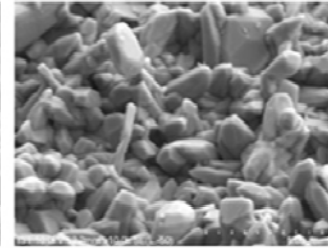
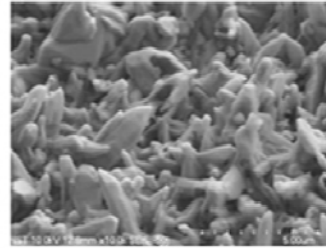
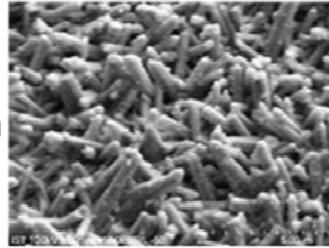
SnPb / NiAu



SAC105 / NiAu

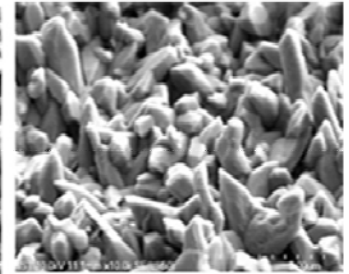
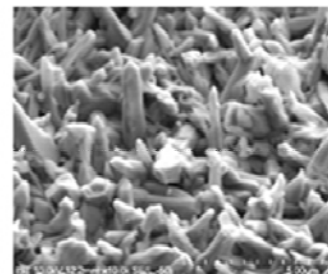
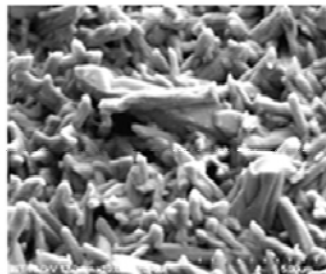
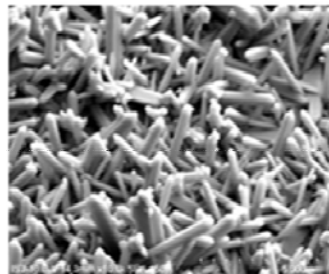


SAC305 / NiAu

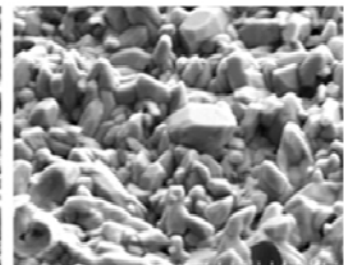
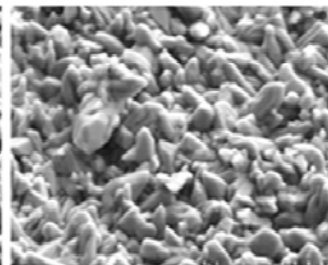
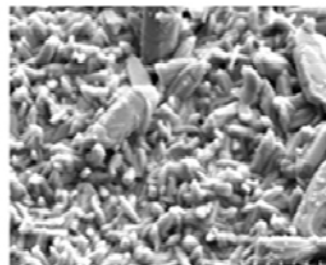
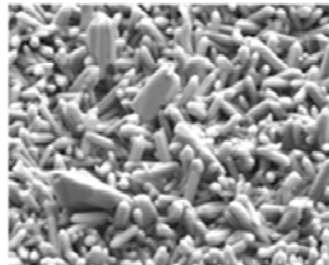


Mn & Ce suppressed
coarsening of IMC rods
at interface

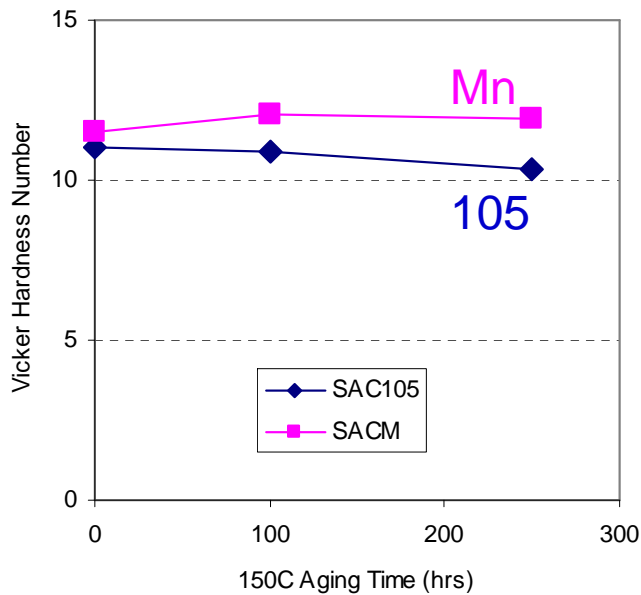
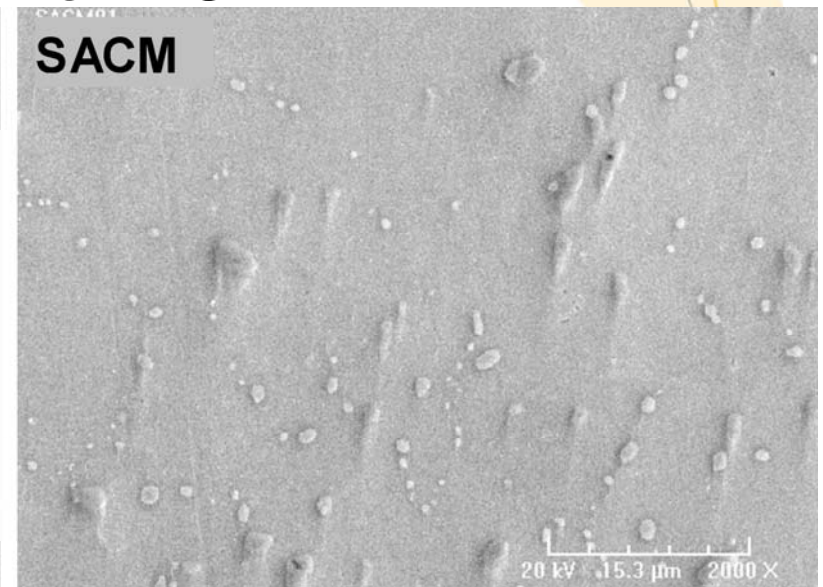
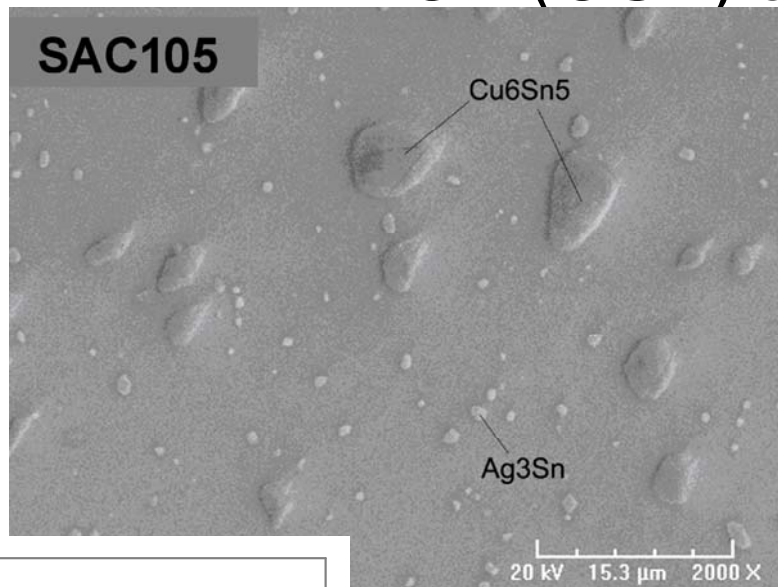
SACM / NiAu



SACC / NiAu



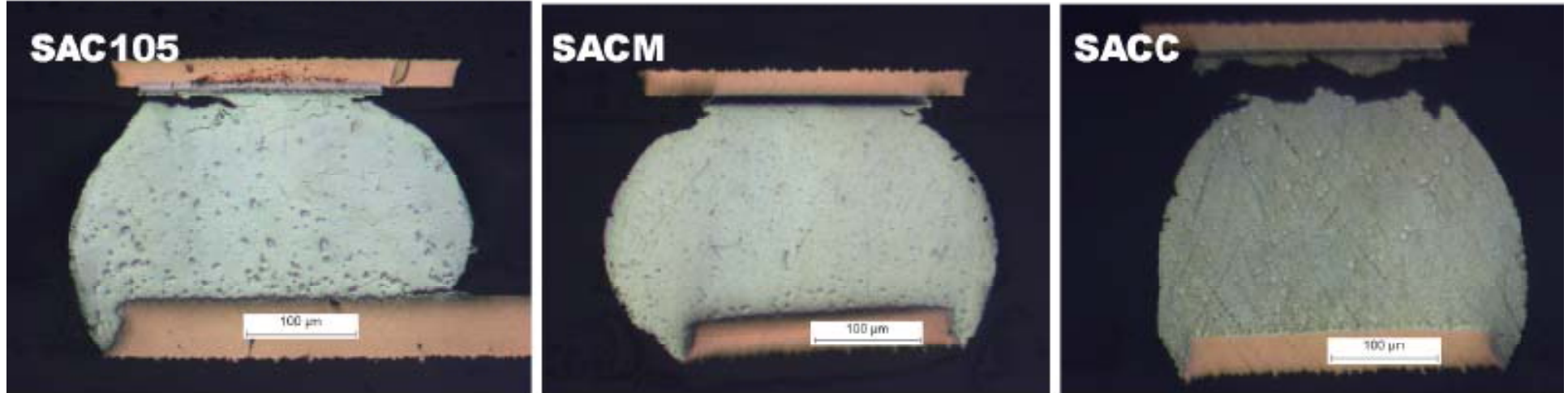
Microstructure of solder joints of TFBGA (NiAu) on PCB (OSP) after TCT



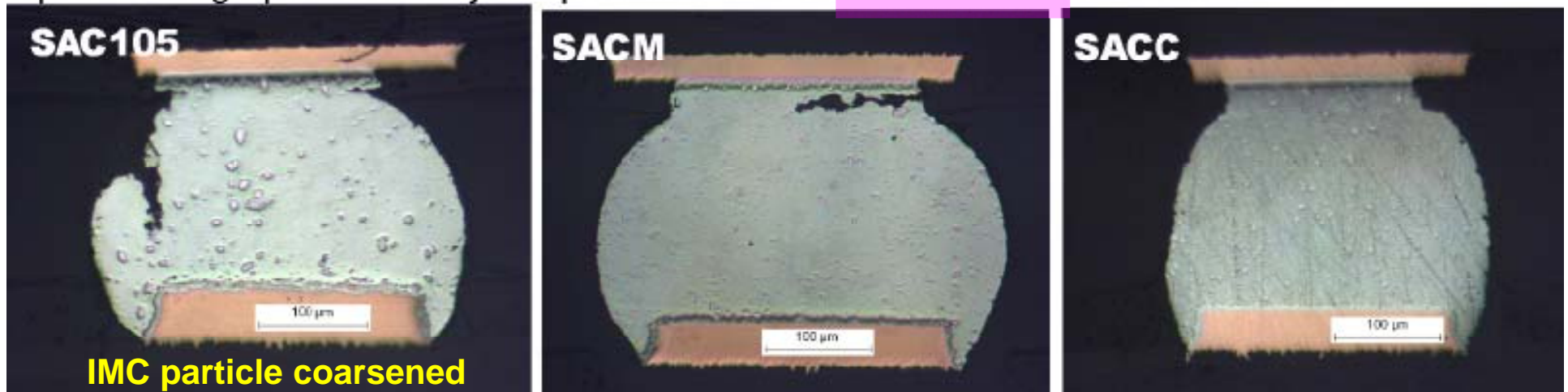
Mn suppressed coarsening of IMC particles, thus maintained hardness of joint

Mn & Ce suppressed IMC coarsening upon thermal aging, hence stabilized microstructure.

Optical micrographs of solder joints after TCT

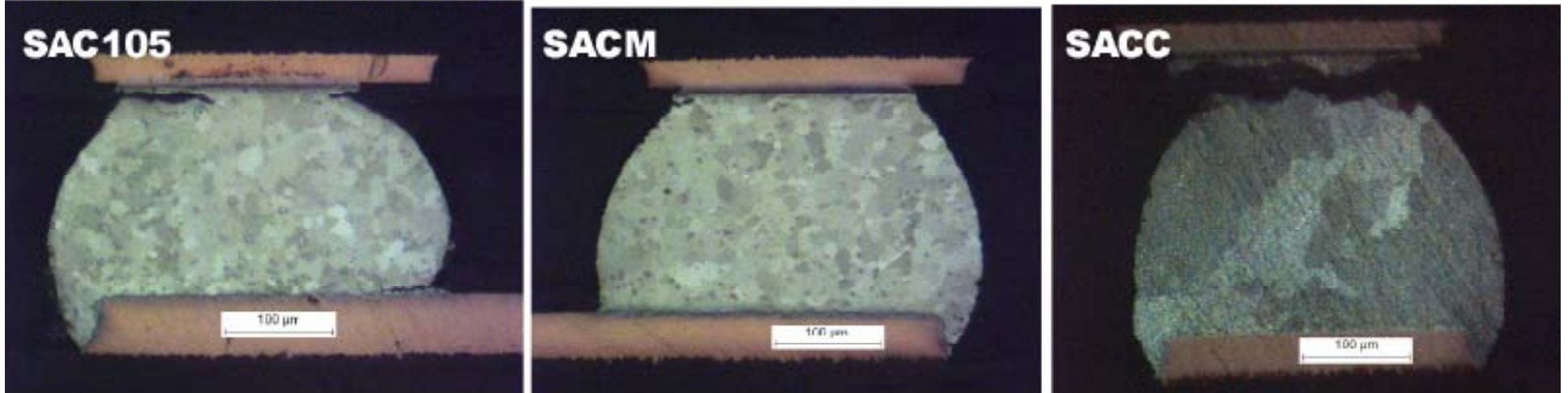


Optical micrographs of solder joints preconditioned at 150°C/250 hrs, followed with TCT



Mn & Ce stabilized grain size upon thermal aging, presumably through stabilizing IMC particles.

Polarized light micrographs of solder joints after TCT



Polarized light micrographs of solder joints preconditioned at 150°C/250 hrs, followed with TCT



Discussion

- Drop Test
 - Both SACM and SACC exhibit **finer and thinner IMC** structure at interface.
- TCT Test
 - A **stable and fine IMC** structure may be the primary contributing factor, and the **stabilized grain** structure resulted may be the secondary cause for SACM and SACC to exhibit a high TCT reliability.

Conclusion

- The Mn or Ce doped low cost SAC105 alloys
 - Achieved a **higher drop test** and **dynamic bending test** reliability than SAC105 and SAC305, and exceeded SnPb for some test conditions.
 - **Matched high Ag SAC in thermal cycling performance**
- The mechanism for high drop performance and high thermal cycling reliability can be attributed to
 - **A stabilized microstructure**, with uniform distribution of fine IMC particles, presumably through the inclusion of Mn or Ce in the IMC.
 - A **thinner IMC** layer
- The cyclic bending results showed SAC305 being the best, and all lead-free alloys are equal or superior to SnPb.
- **BGA package finish: NiAu > OSP** if assembled on PCB (OSP).
- Weak trend on preference of **PCB finishes: ImAg > OSP > ENIG**